THESIS FOR THE DEGREE OF LICENTIATE OF PHILOSOPHY

Some phonons wander by mistake, into the mess where symmetry breaks: Understanding low thermal conductivity by first-principles calculations

DANIEL O. LINDROTH

Department of Physics
CHALMERS UNIVERSITY OF TECHNOLOGY
Göteborg, Sweden 2016

Some phonons wander by mistake,
into the mess where symmetry breaks:
Understanding low thermal conductivity
by first-principles calculations
Daniel O. Lindroth

Department of Physics
Chalmers University of Technology
se-412 96 Göteborg, Sweden
Telephone +46 31 772 10 00

Chalmers reproservice
Göteborg, Sweden 2016

Some phonons wander by mistake, into the mess where symmetry breaks: Understanding low thermal conductivity by first-principles calculations

Daniel O. Lindroth
Department of Physics
Chalmers University of Technology

Abstract

Energy management is arguably one of the most defining challenges for modern societies. An ever increasing demand for energy has to be balanced with the requirement for a sustainable energy economy that minimizes the human impact on the environment. Materials and their ability to transport both electrical and thermal currents play a key role in this area as they are essential components in energy extraction, transport, storage, and consumption technologies. On a microscopic level electrical and thermal transport in materials is governed by its chemical composition as well as the specific arrangement of the constituent atoms. Since relatively small differences in this regard can have a dramatic impact on the macroscopic behavior of a material, a detailed understanding of the underlying processes and couplings is essential for materials development and optimization.

In this thesis the thermal conductivity in two classes of materials of current and future technological importance has been investigated using electronic structure calculations (density functional theory) in combination with methods from statistical physics (Boltzmann transport theory). The first two papers included in this thesis deal with so-called van der Waals solids, layered materials that are currently attracting tremendous attention in the scientific community due their exciting combination of electrical, optical, and thermal properties. The present thesis specifically provides predictions and a detailed analysis of the lattice thermal conductivity in Mo and W-based transition metal dichalcogenides. A model is developed to explain the extreme structure sensitivity of the conductivity and calculations are presented that elucidate chemical trends and establish bounds.

The third paper deals with clathrates, inclusion compounds that have been found to exhibit a combination of transport properties that is very well suited for thermoelectric applications. These materials exhibit extremely small thermal conductivities, which in the present thesis are shown to be caused by a combination of mass effects and very efficient phonon-phonon scattering processes that limit the heat carrying phonon modes to a very small fraction of the total Brillouin zone.

The present thesis provides a stepping stone for future investigations of transport processes in van der Waals solids and clathrates, which eventually should lead to

the development of devices with higher energy efficiency and better materials for energy extraction technologies.

Keywords: thermal conductivity, electronic structure calculations, Boltzmann transport theory, phonons, van der Waals solids, layered compounds, clathrates

LIST OF PUBLICATIONS

This thesis consists of an introductory text and the following papers:

I **Microscopic Origin of Thermal Conductivity Reduction in Disordered van der Waals Solids**
Paul Erhart, Per Hyldgaard and Daniel O. Lindroth
Chemistry of Materials **27**, 5511 (2015)

II **Thermal expansion and transport in van der Waals solids**
Daniel O. Lindroth and Paul Erhart
(In preparation)

III **Chemical order and transport properties in an inorganic clathrate: Optimal structures by computational design**
Mattias Ångqvist, Daniel O. Lindroth and Paul Erhart
(In preparation)

The author's contributions to the papers:

I The author carried out first principles calculations of phonon spectra and the lattice thermal conductivity.

II The author carried out all of the calculations and was the main author of the manuscript.

III The author carried out the calculations of the lattice contribution to the thermal conductivity.

Contents

1 Introduction 1
- 1.1 Energy transport as a challenge . . . 4
- 1.2 Scavenging (waste) heat . . . 4

2 Background 7
- 2.1 Energy . . . 7
- 2.2 Transport theory . . . 8
- 2.3 van der Waals solids . . . 10
- 2.4 Clathrates . . . 11

3 Methodology 13
- 3.1 Boltzmann transport theory . . . 13
  - 3.1.1 The semiclassical assumption . . . 18
  - 3.1.2 The relaxation time approximation . . . 19
  - 3.1.3 Boltzmann transport for electrons in an electric field . . . 20
  - 3.1.4 Boltzmann transport for phonons . . . 22
  - 3.1.5 Lattice thermal conductivity within the RTA . . . 23
  - 3.1.6 Determination of lifetimes . . . 23
    - 3.1.6.1 The perturbed lattice Hamiltonian . . . 23
    - 3.1.6.2 The physical picture . . . 25
    - 3.1.6.3 Lifetimes from first principles . . . 27
- 3.2 Molecular dynamics simulations . . . 27
- 3.3 Atomic forces from first principles . . . 29
- 3.4 Density functional theory . . . 30
  - 3.4.1 The Kohn-Sham ansatz . . . 31
  - 3.4.2 Exchange-correlation functionals . . . 32
  - 3.4.3 van der Waals density functionals . . . 33
  - 3.4.4 Fourier expansion and pseudopotentials . . . 33

4 Summary of the papers 35
- 4.1 Paper I: Ultra-low thermal conductivity in WSe_2 . . . 35

4.2 Paper II: Thermal conductivity in van der Waals solids 37
4.3 Paper III: Thermal conductivity in clathrates 38

5 Outlook **39**

A Liouville's theorem **41**

Acknowledgments **45**

Bibliography **47**

Papers I-III **55**

1

Introduction

Hier spricht die Stimme der Energie,
...
Ich bin Ihr Diener und Ihr Herr zugleich,
Deshalb hütet mich gut.

The Voice of Energy by *Kraftwerk*

It is easy to take energy for granted. At dining tables around the world it is safe to say that the common theme of discussion probably is not the amount of joules needed for enabling the meal at hand. Yet, many joules were spent along the chain from production, to transportation and final preparation.

Energy is such an integral part of our lives that its importance can be hardly overstated, as modern society are entirely dependent on it. On a personal level for water and food, sanitation, transportation, Internet and communication as well as lighting and heating of our homes. The questions concerning the availability of resources for energy production [1], and their stability over time must be considered among the most important questions for our society today and in the future.

So, are there any reasons to worry about the available amount of energy in the future? If one compares the total primary energy supply [2] (TPES) of the world in 1973 to 2013 the supply has roughly doubled from 6.1 Gtoe [3] to 14 Gtoe [2] (Fig. 1.1). At the same time the population has increased from 3.9 to 7.2 billion

[1] Energy production and consumption are here used in the more colloquial sense, not in the sense as a violation of the *first law of thermodynamics* which states that energy can not be created or destroyed, only transformed from one form to another [1].

[2] An estimate of the available primary energy sources in a region.

[3] Giga ton of oil equivalent.

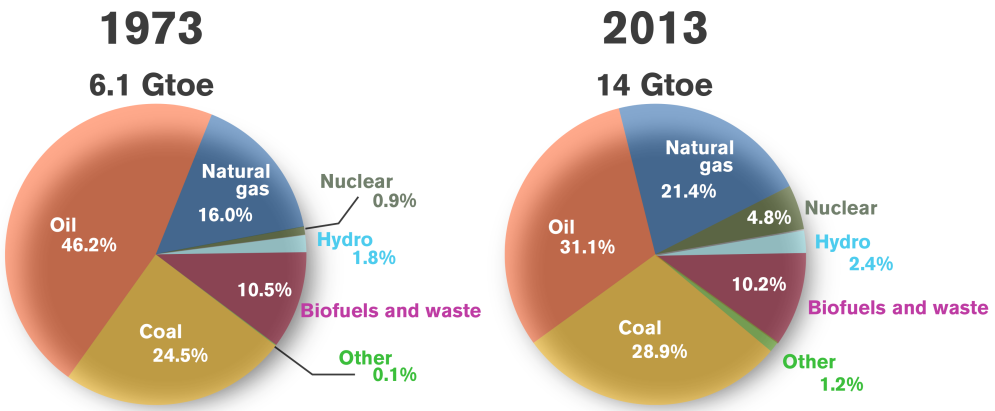

Figure 1.1: Total primary energy supply in the world for different primary energy sources in 1973 and 2013. The data is from the IEA report *Key World Energy Statistics 2015* [2]. The category *Other* includes smaller sources such as geothermal, solar and wind.

people, roughly a doubling as well. There is a strong positive correlation between the world population and the global energy consumption. This can be seen when comparing available data for the world population with the global energy consumption in the span from 1980 to 2012 (Fig. 1.2 (a)). Assuming that the world population is a good estimator for the global energy consumption, up to linear order [4], a linear least squares fit provides a model for estimating the energy consumption based on population size. Using projections of the future world population [4] it is possible to estimate the future energy needs. In a high population scenario the global energy consumption is estimated to steadily increase. Also in a low population scenario the global energy consumption is estimated to increase up until 2050 when it will reach 16 Gtoe after which the demand will start to decline (Fig. 1.2 (b)).

To enable this increase in energy consumption, energy supply must increase as well. In 2013 the global TPES was 81.4 % of the available energy in the form of fossil fuels (coal, oil and natural gas), a small reduction from the 86.2 % in 1973. The oil and gas repositories formed over the last 600 million years [5]. Also coal formed over geological time scales and the fossil fuels are limited resources in that there are finite reserves to extract. Since the reserves are finite the extraction must at some point reach its maximal rate and this sets a physical limit to the possible

[4]There are some deviations from a linear relation connected to economic cycles and stock market crashes. Following the Black Monday stock market crash of October 1987 [3] there is a pause in the growth of global energy consumption during the following years. Similar, in 2009 there is a violation of the linear trend following the stock market crash of 2008.

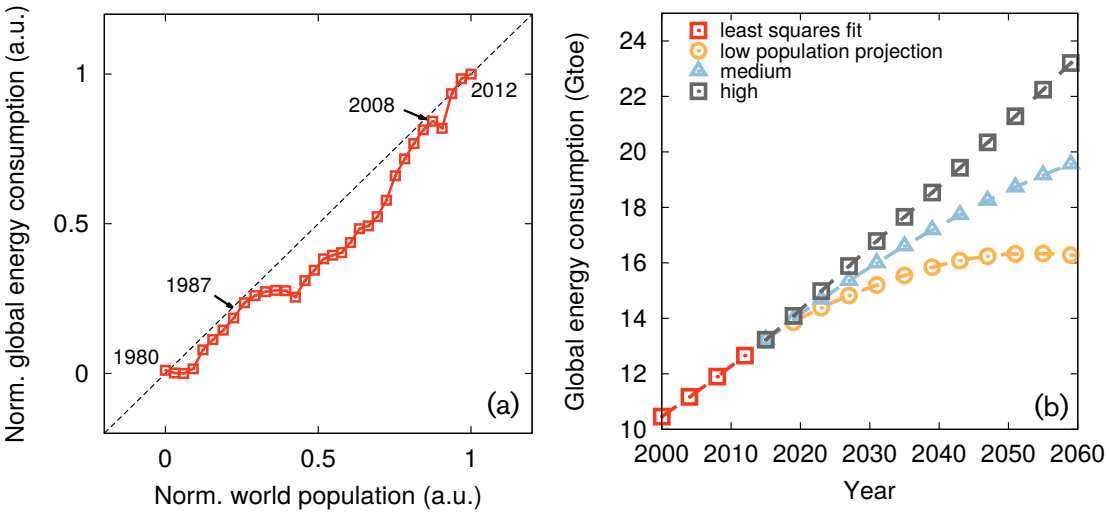

Figure 1.2: (a) Correlation of the world population and yearly total primary energy consumption between the year 1980 and 2011. The data is normalized to the unit interval and received from [4, 10]. (b) Estimations of the future global energy consumption based on three different projections of low, medium and high population growth [4]. The estimates are calculated with a linear model from a least squares fit to the data in the left pane. This gives a connection between yearly energy consumption and the population used in the projections.

supply. The point in time where this happens has been coined *the oil peak* [6, 7]. The term *peak* may be used in the context of any type of finite resource and it is reasonable to talk about *peak coal* and *peak gas* besides *peak oil*. Since the contribution of fossil fuel to the TPES is so dominant there is a real concern if the fossil fuels peak without a realistic alternative at hand. According to the estimate the supply necessarily needs to steadily increase. Although debated, claims that the peak of oil is close have been made [8, 9].

There is another concern in the use of fossil fuels as well. The energy source mainly consists of carbon and combustion results in production of carbon dioxide, CO_2, that is deposited into the atmosphere. Carbon dioxide is a so called greenhouse gas in that it is infrared active. The greenhouse gases allow high frequency sunlight to enter the Earth system, heating the ground without any interference. But since the frequencies of the thermal radiation leaving the Earths surface is shifted to the infrared range, some of the radiation will interact with the greenhouse gases and be trapped in the atmosphere. In effect this results in a reduction of the energy flux out of the Earth system resulting in *Global Warming*. The predicted climate change associated with Global Warming is assumed to present a

future threat if the emission of CO_2 is not reduced in time to halt the increasing mean temperature of the Earth [11].

The dominating position of fossil fuels in the energy economy makes an exchange of the used resources to alternatives based on the current technologies unrealistic in the near future. And although the power of serendipity can be huge, it is an unreliable force. Either way, better administration of fossil fuels is a reasonable strategy to handle either fossil peaks or overconsumption resulting in global warming. Increasing the efficiency of energy consumption e.g., by recuperation of waste heat can make a substantial contribution to the solution of this problem.

1.1 Energy transport as a challenge

The energy stored in fossil fuels can not be used directly, it has to be processed and converted to a form suitable for use. This is a general theme [5] for any kind of utilization of an energy source (Fig. 1.3). There are three fundamental sources of energy [12]. Dominating is energy originating from the sun, followed by nuclear energy and lastly geothermal energy originating from inside the Earth. Fossil fuels originated as energy from the sun accumulating in the biomass from where parts eventually ended up in sedimentary rocks that under the right conditions transformed into coal, oil and gas. To access the stored energy the fuel needs to be combusted and further transformed into a useful form e.g., electricity or mechanical work.

In any type of process involving energy transport or conversion there will be energy dissipation to internal degrees of freedom due to irreversibility [13, 14]. This dissipation will eventually transfer into the surrounding environment resulting in energy losses (Fig. 1.4). The result is a degradation of the energy used as input. For thermal processes these losses are substantial. The disadvantage with dissipated energy is its disordered nature with no clear direction. This makes utilization difficult.

1.2 Scavenging (waste) heat

Because of the dominating position of thermal processes in the economy, technologies that scavenge dissipated energy and thereby raise the overall energy efficiency are of great interest.

Heat engines convert heat into useful, most commonly mechanical or electrical, energy. A specific type of heat engine is the thermoelectric generator (TEG)[15], which converts heat into electrical current by exploiting the thermoelectric effect.

[5] With some exceptions. heating by direct sunlight is one.

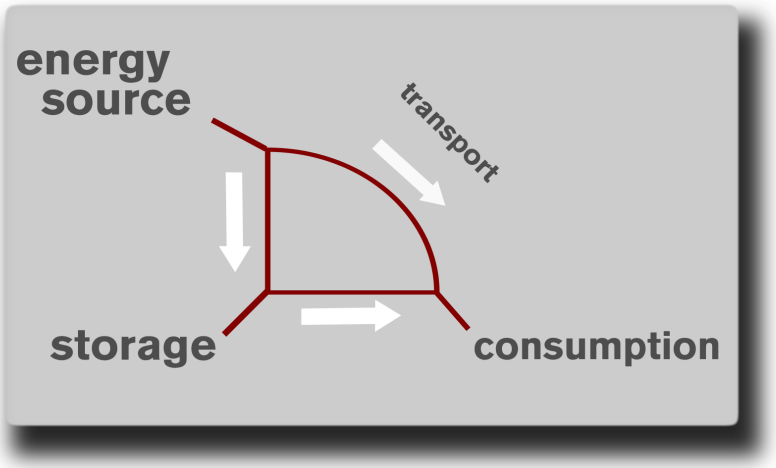

Figure 1.3: Schematic illustration of type of paths from energy source to consumption. After extraction from the energy source it is necessary to store the energy if not directly used. Regardless of the path taken transport processes are present and also one to several types of energy conversion steps.

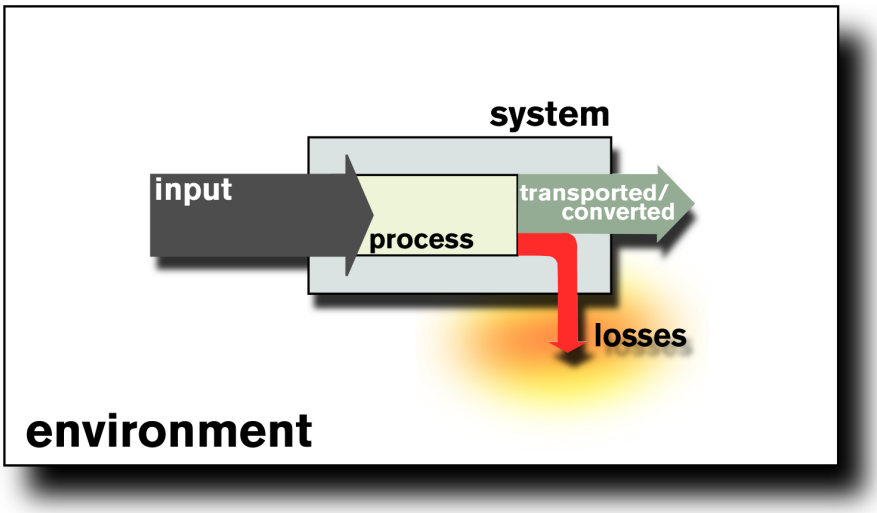

Figure 1.4: Schematics of energy interacting with a system. The energy input is converted and transported through a redirection resulting in useful energy output of transported/converted energy. At the same time, inevitably energy is dissipated to the surrounding environment due to irreversible processes within the system.

The efficiency is here dependent on several factors, one of which is the thermal conductivity with lower values providing better efficiency. To make TEGs economically feasible the efficiency needs to be high enough, higher than it is today. Because of this an understanding how to engineer the thermal conductivity is important.

At the same time, knowledge about how to lower the conductivity can be used to achieve the opposite, namely increasing the conductivity. This has important for heat management in devices. In particular, a high thermal conductivity is particularly important for applications in electronics and opto-electronics to prevent overheating and potential loss of components.

2 Background

2.1 Energy

Most of the energy we utilize originates from the sun, where fusion of hydrogen releases large amounts of energy that reach the Earth in the form of electromagnetic radiation. On Earth the biosphere assimilates the energy mainly through photosynthesis. Historically a lot of this energy has been stored in the form of fossil fuels (oil, coal and natural gas), which formed as the result of geological processes. Besides the sun, we also utilize energy stored in nuclear fuels and to a lesser extent geothermal energy originating from the Earth's core. Solar, nuclear, and geothermal are examples of primary energy sources, that is energy captured directly from the environment. Secondary forms of energy have been derived from a primary source; this includes for example electricity but also fossil as well as synthetic fuels such as gasoline, ethanol and hydrogen [12].

Electricity is often the most useful form of energy in terms of applications. Several processes can be used for transforming different types of energy into electricity, including e.g., electromagnetic induction, the piezoelectric effect, the photoelectric effect, and the thermoelectric effect. Among these, electromagnetic induction dominates as it is the process used in almost all commercial generation of electricity. With respect to this thesis the thermoelectric effect is very interesting because of its importance of low lattice conductivity for the efficiency in thermoelectric materials [15, 16].

2.2 Transport theory

Materials and their ability to transfer charge (electrical currents) and heat (thermal currents) play a key role in energy management as they are essential components in energy extraction, transport, storage, and consumption technologies. On a macroscopic level electrical and thermal conduction in a material can be conveniently described using phenomenological theories e.g., in the form of Ohm's law in the case of electrical conduction and Fourier's law in the case of thermal conduction (see below). The corresponding equations contain transport coefficients such as the electrical conductivity, the Seebeck coefficient, or the thermal conductivity. These are tensorial quantities that are material specific and quantify the response to an external force such as an electric field or a thermal gradient [17].

For example, the thermal conductivity can be phenomenologically defined through Fourier's law

$$\boldsymbol{J} = -\kappa \cdot \nabla T, \tag{2.1}$$

where $\boldsymbol{J}$ is the heat current, which quantifies the rate at which thermal energy is transported as the result of a thermal gradient ∇T, and κ denotes the thermal conductivity tensor.

It is illuminating to examine thermal conductivity from a kinetic point of view as a transport problem in a monatomic gas. To this end, let us assume a stationary thermal gradient in the x-direction. When a particle moves from a region at temperature $T + \Delta T$ to a colder region at temperature T where it thermalizes it needs to give up an energy of $C\Delta T$ from the hotter region to equilibrate, where C is the specific heat. The particle will now be in thermal contact with the new region. Assuming that the length scale for thermalization is ℓ (Fig. 2.1), the expression for the temperature difference is

$$\Delta T = \ell \frac{\partial T}{\partial x}. \tag{2.2}$$

The thermal energy is proportional to the temperature $E \sim T$ and the mean velocity squared $E \sim v^2$. Hence, the mean velocity is proportional to the square root of the temperature and the mean velocity at temperature $T + \Delta T$ is

$$v \sim \sqrt{T + \Delta T} = \sqrt{T}\sqrt{1 + \frac{\Delta T}{T}} \approx \sqrt{T}\left(1 + \frac{1}{2}\frac{\Delta T}{T}\right) = \sqrt{T} + \frac{1}{2}\frac{\Delta T}{\sqrt{T}}. \tag{2.3}$$

For relatively small ΔT the mean velocities are therefore the same.

The particle flux per unit area is given by the mean velocity multiplied with the particle density. The energy flux is then the particle flux multiplied by the average energy ε the particles in the stream are transporting. Over a mean free path ℓ

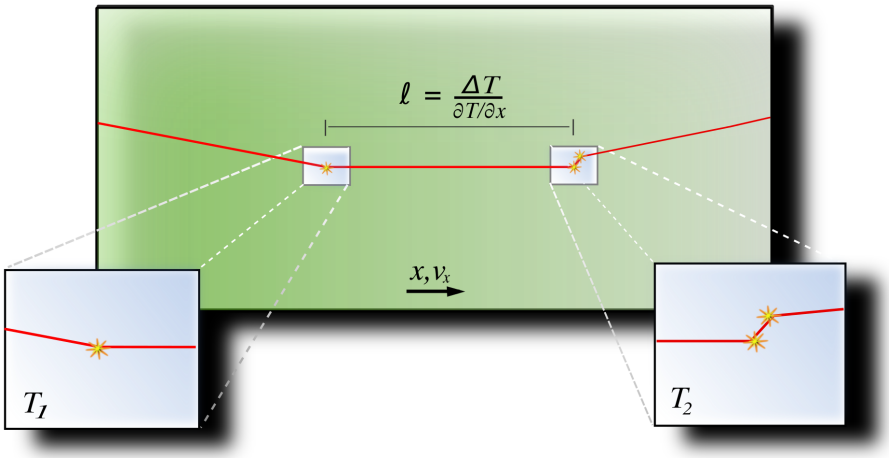

Figure 2.1: The physical picture of the mean free path ℓ in kinetic theory as the length scale between thermalization of a particle propagating in a thermal gradient field.

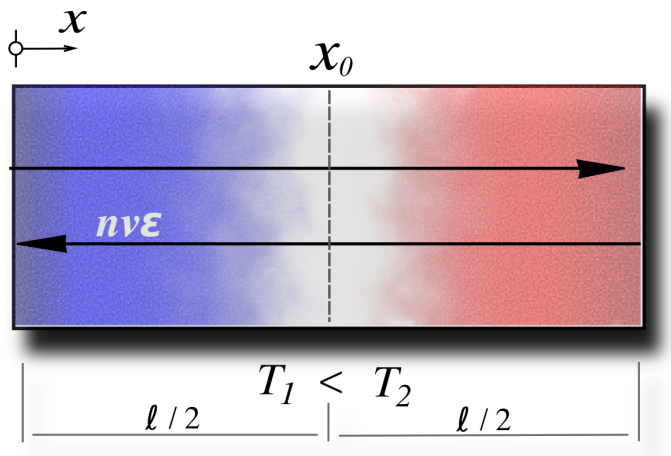

Figure 2.2: The heat flux at x_0 is the net energy flux resulting from ballistic transport over the mean free path ℓ in both directions.

there will be a ballistic transport in both directions. The net flux over the middle of ℓ (Fig. 2.2) is then

$$\begin{aligned} J &= \frac{1}{2} n v \varepsilon \Big|_{x_0 - \ell/2} - \frac{1}{2} n v \varepsilon \Big|_{x_0 + \ell/2} = \frac{1}{2} v \varepsilon \big(n(x_0 - \ell/2) - n(x_0 + \ell/2) \big) \\ &\approx -\frac{1}{2} v \varepsilon \frac{dn}{dx} \ell = -\frac{1}{2} v \ell \frac{d(\varepsilon n)}{dT} \frac{dT}{dx} = -\frac{1}{2} v \ell c \frac{dT}{dx}, \end{aligned} \tag{2.4}$$

where c denotes the specific heat per unit volume. An estimate for the thermal conductivity can then be identified from Fourier's law as

$$\kappa \sim v \ell c. \tag{2.5}$$

This illustrates that the thermal conductivity ought to depend on the mean velocity with which the energy is transported, the length scale for that transport without inelastic scattering as well as the average energy that a carrier transfers.

In this derivation we implicitly assumed local equilibration such that a thermal gradient can be established. This shows that heat is transported downhill with respect to the thermal gradient in accordance with the second law of thermodynamics as stated by Clausius[1]:

No process is possible whose sole result is the transfer of heat from a colder to a hotter body.

For two regions that are thermally connected there will thus always be heat transfer from the hotter to the colder side, unless there is an additional process reversing the heat current.

Equation Eq. (2.5) was derived for a gas of classical particles but can be used to understand the thermal conductivity in solids as well. The heat carriers in solids are electrons and phonons, and the picture above can be adapted by observing that both of these quasi-particles behave as quantum gases for which the correct statistics have to be used. [1]

2.3 van der Waals solids

The term van der Waals solids refers to a class of materials that are composed of layer of different so-called 2D materials such as e.g., graphene, boron nitride (BN), and various transition metal dichalcogenides (TMDs). While intralayer bonding in these materials has usually covalent and/or ionic character, they are coupled

[1] For electrons, which are fermions, Fermi-Dirac statistics apply, whereas phonon as bosons obey Bose-Einstein statistics.

vertically via much weaker van der Waals forces, hence the name. While graphene and boron nitride have been studied in great detail over the years and are increasingly being integrated into devices and applications, TMDs are still primarily in the domain of fundamental research.

Mo and W-based TMDs with the general composition MX_2 (M=Mo,W; X=S,Se,Te) have received the bulk of the attention. With the exception of WTe_2, which has an orthorhombic equilibrium structure, they form structures with hexagonal symmetry (Fig. 2.3).

TMDs in general and Mo and W-based compounds in particular are emerging as promising candidates for a manifold of applications including electronic components [18], optoelectronics [19, 20, 21], thermoelectrics [22], and spintronics [23]. Since thermal transport is relevant for many of these applications, it is important to develop a detailed understanding of thermal transport in these systems.

2.4 Clathrates

Generally, clathrates are chemical substances with a defined lattice structure that can trap atomic or molecular species [24, 25]. Inorganic clathrates e.g., $Ba_8Ga_{16}Ge_{30}$ and $Sr_8Ga_{16}Sn_{30}$, have been found to exhibit very favorable thermoelectric properties due their intrinsic combination of a low thermal conductivity, high Seebeck coefficients, and good dopability [26, 27]. Here, the earth alkaline atoms act as guest species that occupy the cages provided by the host structure, which is most commonly composed of elements from groups 13 and 14. Since the guest atoms in these structures can exhibit "rattler"-like atomic motion due to their relatively small size compared to the available cage [28, 29, 30], they have been linked to the very small lattice thermal conductivity κ_l [31, 32].

Inorganic clathrates of type I belong to space group $Pm\bar{3}n$ (international tables of crystallography number 223) and feature two smaller and six larger cages per unit cell [26, 33, 27]. $Ba_8Ga_{16}Ge_{30}$, which is in the focus of the present work, falls into this category and is representative of many other compounds. It has been investigated extensively both experimentally [34, 35, 36, 37, 38, 39] and theoretically [40, 41, 35, 42, 28], especially because of its promising thermoelectric properties. Here, the host structure is composed of Ga and Ge atoms, which occupy 6*c*, 16*i*, and 24*k* Wyckoff sites [Fig. 2.4] [43] as revealed by experimental measurements of the site occupancy factors [33].

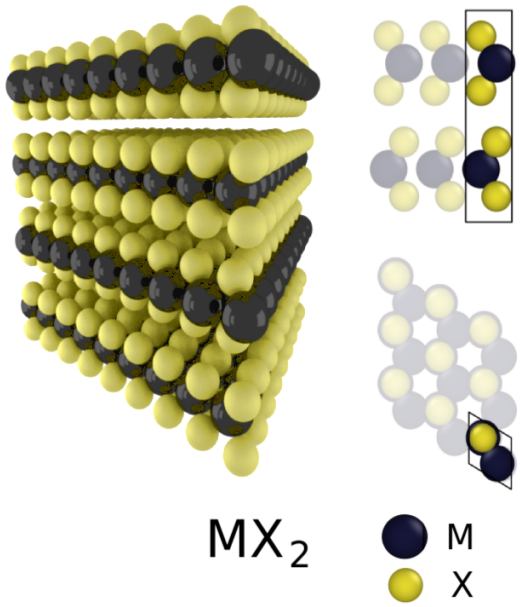

Figure 2.3: The crystal structure of the molybdenum and tungsten based transition metal dichalcogenides. The transition metal corresponds to M and the chalcogenide to X.

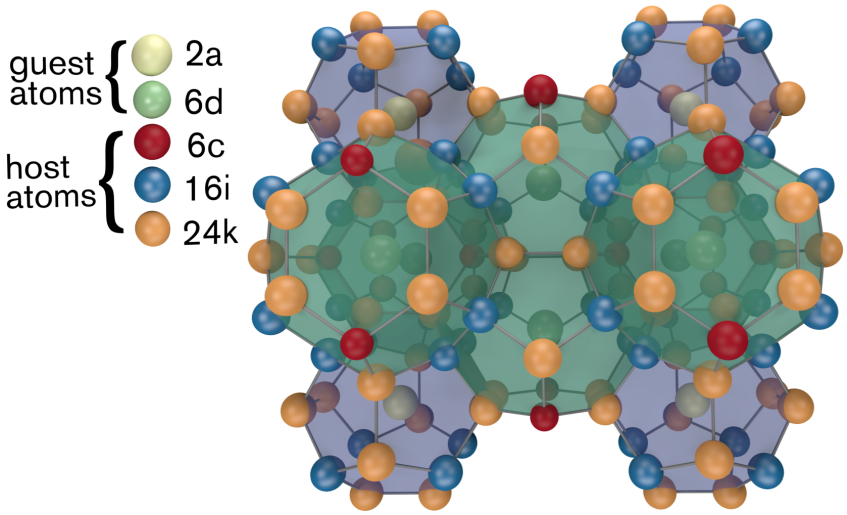

Figure 2.4: Crystal structure of type I clathrates. The guest species (Ba) occupies Wyckoff sites of type 2*a* and 6*d*, while the host species (Ga, Ge) occupy Wyckoff sites of type 6*c*, 16*i*, and 24*k*.

3 Methodology

> The Boltzmann equation is so exceedingly complex that it seems hopeless to expect to generate a solution from it directly.
>
> *J. M. Ziman (1960)*

3.1 Boltzmann transport theory

The book keeping associated with tracking the dynamical variables in one mole of substance is an infeasible task. One attempt at a remedy is to severely reduce the system size, impose suitable boundary conditions and see if this reduction still manages to capture the relevant physics. If this does not work or becomes to difficult an alternative strategy is to abandon exact knowledge of the system and instead give a statistical description. For mechanical systems the concept of distribution functions that tracks the number density over phase space is useful.

The phase space for a system of N particles is $6N$ dimensional where $3N$ of the coordinates corresponds to the different particles generalized positions labeled q_α. The remaining $3N$ degrees of freedom correspond to the different canonical momenta labeled p_α. One can introduce Γ as the set $\{q_1, \dots, q_{3N}, p_1, \dots, p_{3N}\}$ as a specific point in phase space with corresponding volume element $d\Gamma$. A complete description of the dynamical state of a system constitutes then a point Γ. If the system behaves classically[1] and a governing Hamiltonian is known, in principal the

[1] Classical in the sense that the system is well described by Newtonian mechanics.

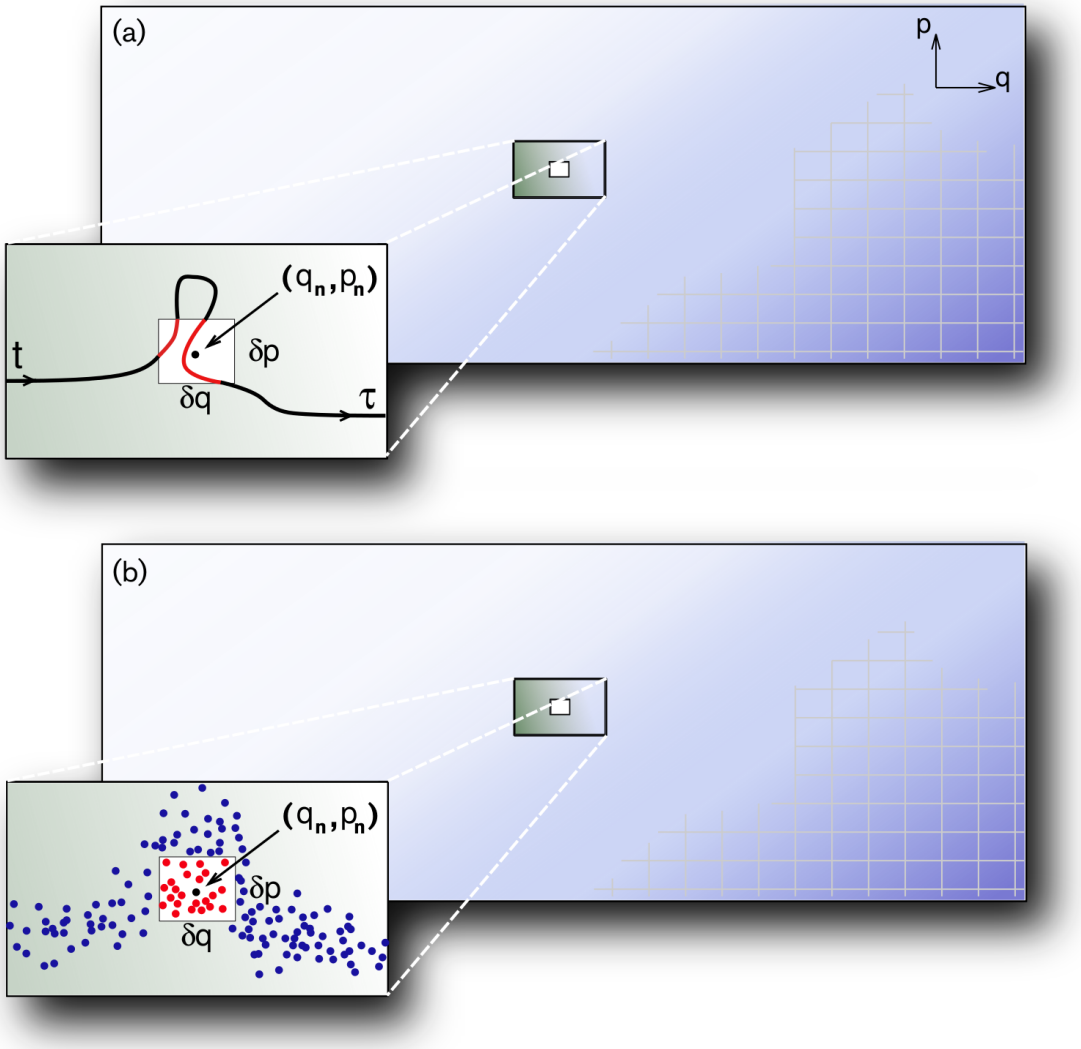

Figure 3.1: Schematic representation of two different views on distribution densities over phase space. (a) Tracking the amount of time a system spends in the neighborhood of a specific phase space point (the red paths) gives a measure for a distribution function. (b) A large enough collection of independent system replicas gives an alternative measure for a distribution function as the ratio between states within a neighborhood to $(\boldsymbol{q}, \boldsymbol{p})$ and all states.

dynamical evolution can be calculated by integrating the canonical equations [44]

$$\begin{aligned} q_\alpha(t) &= \frac{\partial H}{\partial p_\alpha} \\ p_\alpha(t) &= -\frac{\partial H}{\partial q_\alpha} \end{aligned} \tag{3.1}$$

given initial conditions at time t_0. This constitutes $6N$ equations and is an impossible task since N is large, typically at the order of 10^{23} or more for macroscopic systems. In principle though, if the equations were solved the solution would map out a path through the phase space. This can be used to define the notion of a distribution function over the phase space in two different ways.

If a system is observed for a long time τ and the time spent in the neighborhood of a certain point in phase space is denoted as Δt (see Fig. 3.1 (a)), then the limit

$$\rho_N(\Gamma, t)d\Gamma = \lim_{\tau\to\infty} \frac{\Delta t(\Gamma, t)}{\tau} \tag{3.2}$$

defines a N particle probability density $\rho_N(\Gamma)$ corresponding to the uniform probability of finding the system of N particles in a specific state Γ at some time t. Alternatively, one can introduce a large collection constituting independent copies of the system randomly distributed over the phase space. Such a collection is called an ensemble (Fig. 3.1 (b)). One can define the probability density as the ratio between the number of points within the neighborhood of a point Γ and the total number of points.

In appendix A the *Liouville equation* that governs the evolution of ρ is derived. With the use of the Poisson bracket [2] it is written as

$$\frac{d\rho_N}{dt} = \frac{\partial \rho_N}{\partial t} + \{\rho_N, H\} = 0. \tag{3.4}$$

Solving the Liouville equation exactly is an impossible task, but there is some important knowledge gained by its introduction. Due to the conformity to the canonical equations the behavior of the distribution function is that of an incompressible fluid. This has the important implication that a volume element in phase space is invariant in time, a result known as *Liouville's theorem*. The main issue with ρ_N is that it contains to much information. Integrating over all but one of the subspaces,

[2] The Poisson bracket on quantity A is defined as

$$\{A, H\} = \sum_{i=1}^{3N} \left(\frac{\partial A}{\partial q_i}\frac{\partial H}{\partial p_i} - \frac{\partial A}{\partial p_i}\frac{\partial H}{\partial q_i} \right) \tag{3.3}$$

using $d\Gamma_1 = dq_1 dp_1$, produces a new density

$$\rho_1(\boldsymbol{q},\boldsymbol{p},t) = V \int \frac{d\Gamma}{d\Gamma_1} \rho_N(\Gamma) \tag{3.5}$$

called the *one particle density* representing a single particle in the averaged environment of all other particles in the system. The volume V of the system is needed so that the probability of finding the particle in a neighborhood of the six dimensional point $(\boldsymbol{q},\boldsymbol{p})$ is

$$\frac{\rho_1(\boldsymbol{q},\boldsymbol{p})}{V} d\Gamma_1. \tag{3.6}$$

Integrating Liouville's equation over $d\Gamma/d\Gamma_1$ results in

$$\frac{\partial \rho_1}{\partial t} + \{\rho_1, H\} - \left(\frac{\partial \rho_1}{\partial t}\right)\bigg|_{scattering} = 0, \tag{3.7}$$

where the remaining parts of higher order densities have been collected in the last term, subscripted by scattering since this term contains the interaction between the isolated particle and all other particles. Using the canonical equations this may be reformulated in vector form

$$\frac{\partial \rho_1}{\partial t} = - \underbrace{\boldsymbol{v}}_{=\frac{\partial \boldsymbol{q}}{\partial t}} \cdot \nabla \rho_1 - \underbrace{\boldsymbol{F}_{ext.}}_{=\frac{\partial \boldsymbol{p}}{\partial t}} \cdot \nabla_{\boldsymbol{p}} \rho_1 + \left(\frac{\partial \rho_1}{\partial t}\right)\bigg|_{scattering}. \tag{3.8}$$

The first term on the right hand side can be identified with a diffusive process and the second one as influenced by external forces so the equation can be written as

$$\frac{\partial \rho}{\partial t} = \left(\frac{\partial \rho}{\partial t}\right)\bigg|_{diffusion} + \left(\frac{\partial \rho}{\partial t}\right)\bigg|_{external\ fields} + \left(\frac{\partial \rho}{\partial t}\right)\bigg|_{scatt.}. \tag{3.9}$$

This is the *Boltzmann equation* in its general form for a classical distribution of distinguishable particles. It states that the change in the one particle distribution is due to a balance between diffusion, external influence from e.g., electromagnetic or gravitational fields and internal scattering. It is an elegant compact description of the complex situation where external fields accelerate the particles feeding energy into the system shifting the occupation function while scattering events redistribute the energy dissipating it into the structure and relax the perturbed occupation function.

There is an alternative way to derive the Boltzmann equation via Liouville's theorem, that includes some physical intuition. To this end, one starts with neglecting

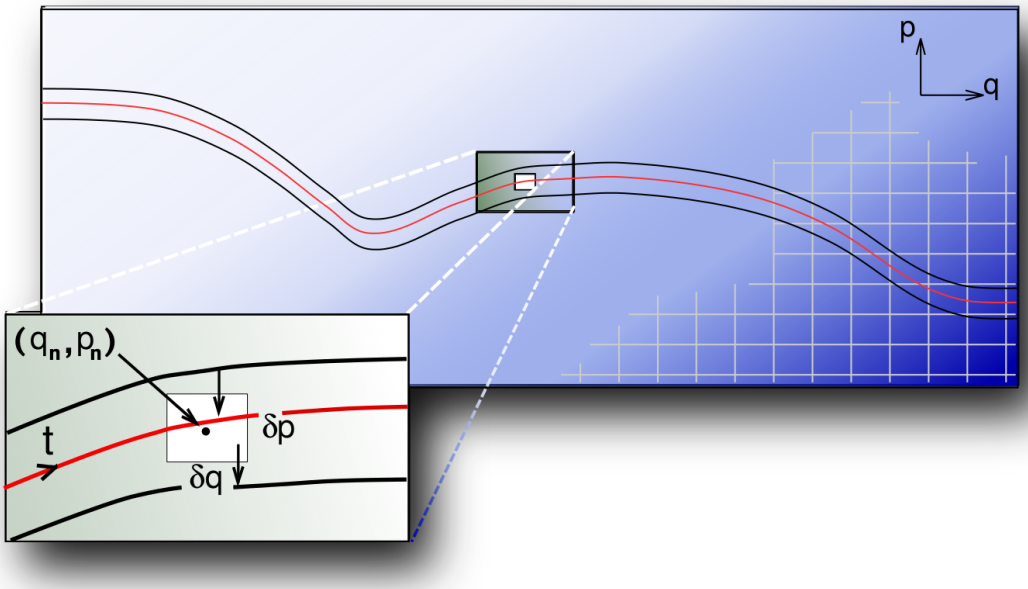

Figure 3.2: Due to scattering processes different paths in phase space may exchange states. Here it is schematically shown how states of certain momenta are scattered into the neighborhood of the path from the top path while states of certain momenta are scattered out of the neighborhood to the bottom path.

scattering, which is reasonable for a sufficiently diluted system. Then one introduces a distribution $f(\boldsymbol{r}, \boldsymbol{p}, t)$ in the form of an occupation function that counts the number of states at $\boldsymbol{r}$ that have momenta $\boldsymbol{p}$ at time t. Because of Liouville's theorem the number of states in a neighborhood of the point at $(\boldsymbol{r}, \boldsymbol{p})$ at time t must all have been transported from another point in accordance with Newton's equations

$$\begin{aligned} d\boldsymbol{r} &= \boldsymbol{v}dt \\ d\boldsymbol{p} &= \boldsymbol{F}dt. \end{aligned} \tag{3.10}$$

Within the neighborhood, using a Taylor expansion the following holds true to first

order in dt

$$\begin{aligned} f(\boldsymbol{r},\boldsymbol{p},t) &= f(\boldsymbol{r}-\boldsymbol{v}dt,\boldsymbol{p}-\boldsymbol{F}dt,t-dt) \\ &= f(\boldsymbol{r},\boldsymbol{p},t) + \left.\frac{\partial f}{\partial r_\alpha}\right|_{(\boldsymbol{r},\boldsymbol{p},t)} v_\alpha dt + \left.\frac{\partial f}{\partial p_\alpha}\right|_{(\boldsymbol{r},\boldsymbol{p},t)} F_\alpha dt + \left.\frac{\partial f}{\partial t}\right|_{(\boldsymbol{r},\boldsymbol{p},t)} dt \end{aligned} \tag{3.11}$$

where the Einstein sum convention applies. Canceling $f(\boldsymbol{r},\boldsymbol{p},t)$, identifying the total derivative and writing the equation in vector notation gives

$$\frac{df}{dt} = \frac{\partial f}{\partial t} + \boldsymbol{v}\cdot\nabla f + \boldsymbol{F}\cdot\nabla_{\boldsymbol{p}} f = 0 \tag{3.12}$$

which must hold in each point of phase-space. Increasing the concentration the particles start to scatter. This means that particles with a certain momentum may be scattered in to a neighboring point in phase space. Alternatively, particles with a certain momentum can scatter out from a neighborhood (Fig. 3.2). This may be expressed symbolically by introducing a transition probability operator $P_{\boldsymbol{p}'\to\boldsymbol{p}}(\boldsymbol{r},\boldsymbol{p})$ giving the rate for states into the phase space point $(\boldsymbol{r},\boldsymbol{p})$. Similarly $P_{\boldsymbol{p}\to\boldsymbol{p}'}$ is the operator that expresses the rate of the states going out from $(\boldsymbol{r},\boldsymbol{p})$ as a result of scattering. Under normal circumstances it is reasonable to assume the principle of detailed balance, which means that in equilibrium the number of states scattered into a phase space point is balanced by an equal amount of states scattered out of the point. The effect of scattering vanishes and so the scattering term disappears. This suggests that the scattering term should appear as the difference of the two transition rates as

$$\boldsymbol{S} = P_{\boldsymbol{p}'\to\boldsymbol{p}} - P_{\boldsymbol{p}\to\boldsymbol{p}'}. \tag{3.13}$$

The rate of states transitioning into and out from the phase space point due to scattering must balance the total change of the occupation function. Including this effect of scattering in Eq. (3.14) the Boltzmann equation becomes

$$\frac{df}{dt} = \frac{\partial f}{\partial t} + \boldsymbol{v}\cdot\nabla f + \boldsymbol{F}\cdot\nabla_{\boldsymbol{p}} f = \boldsymbol{S}f. \tag{3.14}$$

3.1.1 The semiclassical assumption

The Boltzmann equation Eq. (3.14) may be rewritten using the quantum mechanical expression for the crystal momentum $\boldsymbol{p} = \hbar\boldsymbol{k}$

$$\frac{df}{dt} = \frac{\partial f}{\partial t} + \boldsymbol{v}\cdot\nabla f + \frac{\boldsymbol{F}}{\hbar}\cdot\nabla_{\boldsymbol{k}} f = \left.\left(\frac{\partial f}{\partial t}\right)\right|_{scattering}. \tag{3.15}$$

The appearance of $\hbar$ indicates that the equation may be applied in a quantum mechanical setting under certain conditions.

The distribution function needs to take into account that particles are indistinguishable. This is accomplished by letting the equilibrium distribution function describe either bosonic or fermionic statistics. In practice this means that the equilibrium distribution is either the Bose-Einstein or the Fermi-Dirac distribution.

In the quantum mechanical description the particles are described by wavefunctions. This has the implication that the velocity appearing in Eq. (3.15) is identified with the group velocity of the waves associated with the states in f. Particle position and momentum then cannot be determined simultaneously with arbitrary precision. Being conjugate operators with a non-vanishing commutator the uncertainty principle limits the precision to

$$\Delta x \Delta p \geq \hbar. \tag{3.16}$$

This is fine as long as Δx can be taken large enough to ensure low uncertainty in p. Since $\hbar$ is of the order 10^{-34} Js a granular view of x may be sufficient and still produce enough precision for the Boltzmann equation. The granularity is sufficient as long as the spatial extent of the wave packet is on a scale less than the mean free path between particle collisions.

According to the *Ehrenfest Theorem* the center of a wavepacket follows the path of a classical particle in a potential [45]. If the wavepacket is sufficiently localized on the scale of the potential the particle may, to a good approximation, be viewed as a classical particle in that potential. This has the implication that the potential must be slowly varying on the length scale of the wave packet. For time varying fields this also sets a temporal constraint so that the frequency associated with the time variation of the field may not become to large.

This is the basis for the semiclassical assumption and restricts the application of the Boltzmann equation to situations, in which quantum interference is not expected.

3.1.2 The relaxation time approximation

The scattering term in Eq. (3.14) is in general a complicated operator. Assuming that there are no external fields and that the system is spatially homogeneous the Boltzmann equation reads

$$\frac{\partial f}{\partial t} = \boldsymbol{S} f. \tag{3.17}$$

If we assume that the system is close to equilibrium the distribution function should be the equilibrium distribution f_0 with an added small perturbation formally writ-

ten as

$$\delta f = f - f_0. \tag{3.18}$$

If the internal scattering is assumed to relax the system, the simplest way to model this is to assume that the rate of change in the distribution function is reduced by the magnitude of the perturbation to the state, over a time scale τ. Equation 3.17 then becomes

$$\frac{\partial f}{\partial t} = \frac{\partial(\delta f)}{\partial t} = -\frac{\delta f}{\tau}. \tag{3.19}$$

with the solution

$$\delta f = \delta f(0) e^{-t/\tau} \tag{3.20}$$

indicating exponential decay of the perturbations over a characteristic time τ. It is natural to call this the relaxation time and the inclusion of the scattering term as in Eq. (3.20) for the *relaxation time approximation* (RTA).

3.1.3 Boltzmann transport for electrons in an electric field

As an example of a solution to the Boltzmann equation within the RTA the case of electrons in a static electric field is presented in this section. The next section considers the Boltzmann equation for phonons in a thermal gradient.

Electrons are fermions and as such obey *Fermi-Dirac* statistics. This is a result of the *Pauli exclusion principle*, which states that two fermions can not simultaneously be in the same quantum state. The occupation in thermal equilibrium at temperature T is then described by the Fermi-Dirac distribution

$$f_0 = \frac{1}{\exp\left(\frac{\varepsilon-\mu}{k_B T}\right) + 1}, \tag{3.21}$$

where ε is the energy of an electron with wave vector $\boldsymbol{k}$ and μ is the chemical potential of the electrons.

If a static electric field $\boldsymbol{E}$ is applied to the material the electrons will experience a Coulomb force accelerating them in the direction opposite to the the electric field. If the fundamental charge is q then the force on the electrons will be $\boldsymbol{F} = -q\boldsymbol{E}$. The electron energy and the chemical potential will then become spatially dependent. Assuming that the RTA holds in the steady state the Boltzmann transport equation is stated as

$$\frac{df}{dt} = \underbrace{\frac{\partial f}{\partial t}}_{=0} + \boldsymbol{v} \cdot \nabla f - \frac{q\boldsymbol{E}}{\hbar} \cdot \nabla_{\boldsymbol{k}} f = -\frac{\delta f}{\tau}. \tag{3.22}$$

If the perturbations are small compared to f_0 the variation in δf will be negligible compared to variations in f. The gradients of δf may then be dropped and the equation becomes

$$\boldsymbol{v} \cdot \nabla f_0 - \frac{q\boldsymbol{E}}{\hbar} \cdot \nabla_{\boldsymbol{k}} f_0 = -\frac{\delta f}{\tau}. \tag{3.23}$$

The perturbations may then be solved for algebraically as

$$\delta f = -\tau \left(\boldsymbol{v} \cdot \nabla f_0 - \frac{q\boldsymbol{E}}{\hbar} \cdot \nabla_{\boldsymbol{k}} f_0 \right). \tag{3.24}$$

Since the equilibrium distribution is known, this presents a full solution within the RTA up to the free parameters in the form of the relaxation times τ. These parameters must be measured, estimated or calculated from first principles.

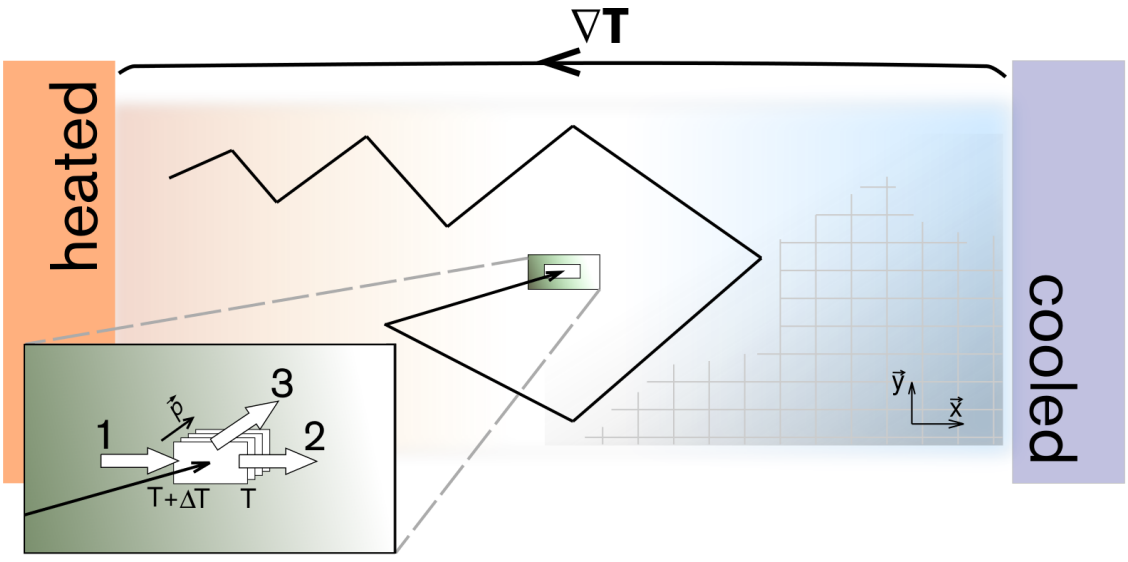

Figure 3.3: A particle experiencing several scattering events here shown in position space.

3.1.4 Boltzmann transport for phonons

In a crystal in thermal equilibrium at temperature T the phonon modes are distributed according to the Bose-Einstein distribution [17]

$$n_{0,\lambda} = \frac{1}{\exp\left(\hbar\omega_\lambda / k_B T\right) - 1}. \tag{3.25}$$

The distribution function counts the number of phonon modes in state λ. Here $\lambda = (\boldsymbol{q}, p)$ is a collective index for a phonon mode with wave-vector $\boldsymbol{q}$ and band index p. The energy carried by a single phonon mode λ is

$$E_\lambda = \frac{\hbar\omega_\lambda}{\exp\left(\hbar\omega_\lambda / k_B T\right) - 1}. \tag{3.26}$$

The specific heat c_λ associated with phonon mode λ is then

$$c_\lambda = \frac{\partial E_\lambda}{\partial T} = k_B \left(\frac{\hbar\omega_\lambda}{k_B T}\right)^2 n_{0,\lambda}(n_{0,\lambda} + 1). \tag{3.27}$$

When there is a thermal gradient present the temperature becomes position dependent. The phonons in question are assumed not to interact with the electromagnetic field and so the force related term drops out. Then in the steady state only the diffusive term from the total derivative survives

$$\frac{dn_\lambda}{dt} = \underbrace{\frac{\partial n_\lambda}{\partial t}}_{=0} + \boldsymbol{v}_\lambda \cdot \nabla n_\lambda + \underbrace{\boldsymbol{F}\frac{\partial n_\lambda}{\partial p}}_{=0} = \left(\boldsymbol{v}_\lambda \cdot \nabla T(\boldsymbol{r})\right)\frac{\partial n_{0,\lambda}}{\partial T}. \tag{3.28}$$

where in the second step the diffusive term has been linearized. Introducing the scattering operator $\boldsymbol{S}$ acting on the distribution the linearized phonon Boltzmann equation in its *canonical form* reads

$$-\left(\boldsymbol{v}_\lambda \cdot \nabla T(\boldsymbol{r})\right)\frac{\partial n_{0,\lambda}}{\partial T} + \boldsymbol{S}n_\lambda = 0 \tag{3.29}$$

emphasizing the balance between diffusion and scattering in a specific mode. So there is thus a balance between a diffusive process and scattering. Introducing the RTA the scattering term is

$$\boldsymbol{S}n_\lambda = -\frac{n_\lambda - n_{0,\lambda}}{\tau_\lambda} = -\frac{\delta n_\lambda}{\tau_\lambda}. \tag{3.30}$$

and solving for the perturbation gives the solution

$$\delta n_\lambda = -\tau_\lambda\left(\boldsymbol{v}_\lambda \cdot \nabla T(\boldsymbol{r})\right)\frac{\partial n_{0,\lambda}}{\partial T} = -\tau_\lambda\left(\boldsymbol{v}_\lambda \cdot \nabla T(\boldsymbol{r})\right)\frac{\hbar\omega_\lambda}{k_B T^2} n_{0,\lambda}(n_{0,\lambda} + 1). \tag{3.31}$$

for a specific phonon mode λ.

3.1.5 Lattice thermal conductivity within the RTA

The microscopic thermal energy current $\boldsymbol{J}_Q$ resulting from phonon transport is the sum of the occupation weighted energy flux of individual phonon modes. The heat flux in the Cartesian direction α is

$$J_{Q,\alpha} = \frac{1}{V}\sum_{\lambda} \hbar\omega_\lambda n_\lambda \boldsymbol{v}_{\lambda,\alpha} = \frac{1}{V}\sum_{\lambda} \hbar\omega_\lambda \delta n_\lambda \boldsymbol{v}_{\lambda,\alpha}. \tag{3.32}$$

Here V is the volume of the system under consideration, ω_λ is the frequency, n_λ is the occupation and $\boldsymbol{v}_\lambda = \nabla_{\boldsymbol{q}}\omega_\lambda$ the group velocity. In the second step the distribution has been replaced with the perturbation. This is because of time reversal symmetry. In equilibrium there will be no energy current since each phonon mode will have an associated mode with an equally energetic phonon in the opposite direction. The terms in Eq. (3.32) cancels in pairs.

Inserting the solution (3.31) in Eq. (3.32) gives an expression for the heat current

$$\begin{aligned} J_{Q,\alpha} &= -\frac{1}{V}\sum_{\lambda} \tau_\lambda \left(v_{\lambda,\beta}\partial_\beta T\right) \underbrace{k_B\left(\frac{\hbar\omega_\lambda}{k_B T}\right)^2 n_{0,\lambda}\left(n_{0,\lambda}+1\right)}_{=\, c_\lambda} \\ &= -\Big(\underbrace{\frac{1}{V}\sum_{\lambda} \tau_\lambda v_{\lambda,\alpha} v_{\lambda,\beta} c_\lambda)}_{=\, \kappa_{\alpha,\beta}(T)} \Big)\partial_\beta T \\ &= -\kappa_{\alpha,\beta}(T)\partial_\beta T \end{aligned} \tag{3.33}$$

where repeated Cartesian index β is implicitly summed. The introduced quantity $\kappa_{\alpha,\beta}$ can be identified through Fourier's law

$$\boldsymbol{J}_Q = -\kappa \cdot \nabla T \tag{3.34}$$

as the thermal conductivity tensor. The expression for the lattice thermal conductivty has one flaw. It contains free parameters in the τ_λ.

3.1.6 Determination of lifetimes

3.1.6.1 The perturbed lattice Hamiltonian

If a unit cell has the position vector $\boldsymbol{l}$ and an atom in that cell has the relative position $\boldsymbol{b}$ the position of the atom may be denoted $\boldsymbol{r}(\boldsymbol{lb})$, where $\boldsymbol{l}$ and $\boldsymbol{b}$ label the atom, and a displacement of this atom will then be

$$\boldsymbol{u}(\boldsymbol{lb}) = \boldsymbol{r}(\boldsymbol{lb}) - \boldsymbol{l} - \boldsymbol{b}. \tag{3.35}$$

For small displacements in a classical crystal the change in the potential energy can be expressed as a Taylor series in the displacements. Formally this is expressed as

$$\begin{aligned} U = U_0 &+ \sum_{\boldsymbol{lb}} \left.\frac{\partial U}{\partial u^\alpha(\boldsymbol{lb})}\right|_0 u_\alpha(\boldsymbol{lb}) \\ &+ \frac{1}{2}\sum_{\boldsymbol{lb}}\sum_{\boldsymbol{l'b'}} \left.\frac{\partial^2 U}{\partial u^\alpha(\boldsymbol{lb})\partial u^\beta(\boldsymbol{l'b'})}\right|_0 u_\alpha(\boldsymbol{lb})u_\beta(\boldsymbol{l'b'}) \\ &+ \frac{1}{6}\sum_{\boldsymbol{lb}}\sum_{\boldsymbol{l'b'}}\sum_{\boldsymbol{l''b''}} \left.\frac{\partial^3 U}{\partial u^\alpha(\boldsymbol{lb})\partial u^\beta(\boldsymbol{l'b'})\partial u^\gamma(\boldsymbol{l''b''})}\right|_0 u_\alpha(\boldsymbol{lb})u_\beta(\boldsymbol{l'b'})u_\gamma(\boldsymbol{l''b''}) + \dots \,. \end{aligned} \tag{3.36}$$

The repeated Greek indices, representing Cartesian directions, are implicitly summed over in pairs. The derivatives are taken at the equilibrium positions, hence the first order term vanishes by definition and the constant term is an arbitrary shift of the energy scale and is here chosen as the reference. Since force is the spatial derivative of the potential the first type of derivative can be rewritten as

$$\Phi_{\alpha\beta}(\boldsymbol{lb},\boldsymbol{l'b'}) = \left.\frac{\partial^2 U}{\partial u^\alpha(\boldsymbol{lb})\partial u^\beta(\boldsymbol{l'b'})}\right|_0 = -\left.\frac{\partial F_\beta(\boldsymbol{l'b'})}{\partial u^\alpha(\boldsymbol{lb})}\right|_0 \tag{3.37}$$

with the physical interpretation as the change in the force on the atom at $\boldsymbol{l'b'}$ as a response when atom $\boldsymbol{lb}$ is displaced. Similarly for the third order term

$$\Phi_{\alpha\beta\gamma}(\boldsymbol{lb},\boldsymbol{l'b'},\boldsymbol{l''b''}) = \left.\frac{\partial^3 U}{\partial u^\alpha(\boldsymbol{lb})\partial u^\beta(\boldsymbol{l'b'})\partial u^\gamma(\boldsymbol{l''b''})}\right|_0 = -\left.\frac{\partial^2 F_\gamma(\boldsymbol{l'b'})}{\partial u^\alpha(\boldsymbol{lb})\partial u^\beta(\boldsymbol{l'b'})}\right|_0 \tag{3.38}$$

relating the displacements of atoms to the force on atom $\boldsymbol{l''b''}$ when displacing atoms $\boldsymbol{lb}$ and $\boldsymbol{l'b'}$. These sets of constants are called the second and third order interatomic force constants (IFC). Up to third order the potential is expressed as

$$U = \frac{1}{2}\sum_{\boldsymbol{lb}} \Phi_{\alpha\beta}u_\alpha(\boldsymbol{lb})u_\beta(\boldsymbol{l'b'}) + \frac{1}{6}\sum_{\boldsymbol{lb}}\sum_{\boldsymbol{l'b'}} \Phi_{\alpha\beta\gamma}u_\alpha(\boldsymbol{lb})u_\beta(\boldsymbol{l'b'})u_\gamma(\boldsymbol{l''b''}). \tag{3.39}$$

Through quantization by introduction of creation and annihilation operators $a_{\boldsymbol{q},s}$ and $a^\dagger_{-\boldsymbol{q},s}$ the displacements may be promoted to operators expressed through the Fourier expansion

$$u_\alpha(\boldsymbol{lb}) = \frac{1}{\sqrt{N}}\sum_{\boldsymbol{lb}} \epsilon_{s,\alpha}(\boldsymbol{q})e^{-i\boldsymbol{q}\cdot\boldsymbol{r}(\boldsymbol{lb})}\sqrt{\frac{\hbar}{2m_{\boldsymbol{b}}\omega_s(\boldsymbol{q})}}\left(\hat{a}_{\boldsymbol{q},s} + \hat{a}^\dagger_{-\boldsymbol{q}s}\right), \tag{3.40}$$

where $\epsilon_{s,\alpha}(\boldsymbol{q})$ is the polarization of the mode and $m_{\boldsymbol{b}}$ the mass of the atom at position $\boldsymbol{b}$. Using this expansion the first sum in Eq. (3.39) together with the kinetic energy can be shown to give a Hamiltonian

$$H_0 = \sum_{\boldsymbol{q},s} \hbar\omega_s(\boldsymbol{q}) \left(\frac{1}{2} + \hat{a}^\dagger_{\boldsymbol{q},s} \hat{a}_{-\boldsymbol{q},s} \right) \tag{3.41}$$

that is the same as the sum of Hamiltonians for quantum harmonic oscillators. This Hamiltonian acts as an unperturbed state constituting a set of harmonic oscillators and the second series acts as a perturbation on that set. The Hamiltonian extended to the third order in the displacements may be written as

$$H^{(3)} = H_0 + H' \tag{3.42}$$

where

$$H' = \frac{1}{6} \sum_{\boldsymbol{lb}} \sum_{\boldsymbol{l'b'}} \sum_{\boldsymbol{l''b''}} \Phi_{\alpha\beta\gamma} u_\alpha(\boldsymbol{lb}) u_\beta(\boldsymbol{l'b'}) u_\gamma(\boldsymbol{l''b''}). \tag{3.43}$$

3.1.6.2 The physical picture

To understand the physical meaning of the perturbed Hamiltonian notice that there are three displacements containing the sum of a creation and an annihilation operator in the third order term in Eq. (3.39). Introducing a phonon field represented by a state-vector with the occupation of individual phonon modes

$$\phi = |n_{\boldsymbol{q}_1,s_1}, n_{\boldsymbol{q}_2,s_2}, \ldots\rangle, \tag{3.44}$$

where the excitations are harmonic oscillators. The creation and annihilation operators then work such that the annihilation operator lowers the phonon occupation $n_{\boldsymbol{q},s}$ by one phonon

$$\hat{a}_{\boldsymbol{q},s} | \ldots, n_{\boldsymbol{q},s}, \ldots\rangle \propto | \ldots, n_{\boldsymbol{q},s} - 1, \ldots\rangle, \tag{3.45}$$

and the creation operator raises the occupation by one phonon

$$\hat{a}^\dagger_{-\boldsymbol{q},s} | \ldots, n_{\boldsymbol{q},s}, \ldots\rangle \propto | \ldots, n_{\boldsymbol{q},s} + 1, \ldots\rangle. \tag{3.46}$$

Expanding the factors containing sums of creation and annihilation operators gives the following factors

$$\begin{aligned} \left(\hat{a}_{\boldsymbol{q},s} + \hat{a}^\dagger_{-\boldsymbol{q},s} \right) \left(\hat{a}_{\boldsymbol{q}',s'} + \hat{a}^\dagger_{-\boldsymbol{q}',s'} \right) \left(\hat{a}_{\boldsymbol{q}'',s''} + \hat{a}^\dagger_{-\boldsymbol{q}'',s''} \right) = \\ \hat{a}_{\boldsymbol{q},s} \hat{a}_{\boldsymbol{q}',s'} \hat{a}_{\boldsymbol{q}'',s''} + \hat{a}_{\boldsymbol{q},s} \hat{a}_{\boldsymbol{q}',s'} \hat{a}^\dagger_{\boldsymbol{q}'',s''} + \hat{a}_{\boldsymbol{q},s} \hat{a}^\dagger_{\boldsymbol{q}',s'} \hat{a}_{\boldsymbol{q}'',s''} + \hat{a}_{\boldsymbol{q},s} \hat{a}^\dagger_{\boldsymbol{q}',s'} \hat{a}^\dagger_{\boldsymbol{q}'',s''} \\ + \hat{a}^\dagger_{\boldsymbol{q},s} \hat{a}_{\boldsymbol{q}',s'} \hat{a}_{\boldsymbol{q}'',s''} + \hat{a}^\dagger_{\boldsymbol{q},s} \hat{a}^\dagger_{\boldsymbol{q}',s'} \hat{a}_{\boldsymbol{q}'',s''} + \hat{a}^\dagger_{\boldsymbol{q},s} \hat{a}_{\boldsymbol{q}',s'} \hat{a}^\dagger_{\boldsymbol{q}'',s''} + \hat{a}^\dagger_{\boldsymbol{q},s} \hat{a}^\dagger_{\boldsymbol{q}',s'} \hat{a}^\dagger_{\boldsymbol{q}'',s''}. \end{aligned} \tag{3.47}$$

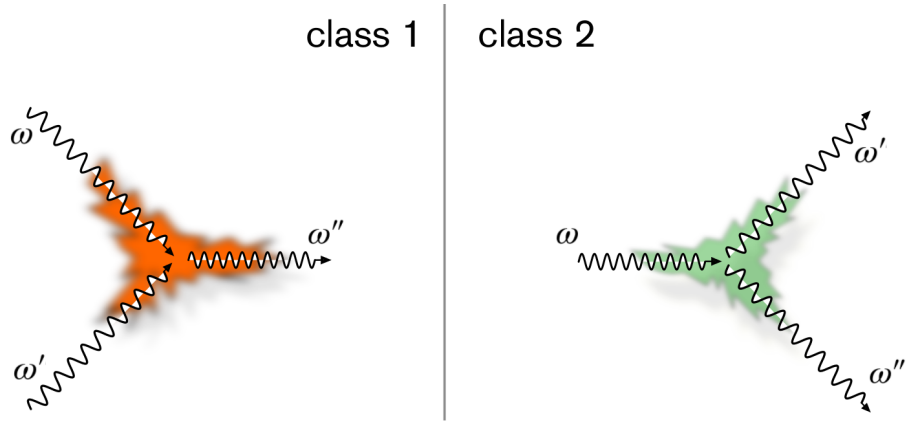

Figure 3.4: Schematic representation of class 1 and class 2 events. Class 1 events corresponds to the collision of two phonons with angular frequency ω and ω' annihilating into a phonon of angular frequency ω''. Class 2 events corresponds to the disintegration of a phonon mode of angular frequency ω annihilating into two phonons with angular frequency ω' and ω''.

Four different kinds of processes can be identified. One with three created phonons, one with three annihilated phonons, two created phonons annihilated into one phonon, and finally one created phonon annihilating into two phonons. The situation with only created or annihilated phonons are prohibited due to energy conservation and do not represent physical processes. Situations in which two phonons collide are called class 1 events and situations in which one phonon disintegrates into two new phonons are called class 2 events (Fig. 3.4). Energy conservation also applies to class 1 and 2 events. This can be expressed through factors of Dirac delta functions expressing energy conservation, $\delta(\omega + \omega' - \omega'')$ for class 1 events and $\delta(\omega - \omega' - \omega'')$ for class 2 events.

Besides energy conservation it is also necessary for the processes to respect the conservation of crystal momentum. A crystal in rest does not have any external momentum but the internal degrees of freedom are associated with a related quantity referred to as crystal momentum. But there is one difference, the crystal momentum must only be conserved up to a reciprocal lattice vector. This can be written as

$$\boldsymbol{q} + \boldsymbol{q}' = \boldsymbol{q}'' + \boldsymbol{G}, \tag{3.48}$$

for class 1 events and

$$\boldsymbol{q} + \boldsymbol{G} = \boldsymbol{q}' + \boldsymbol{q}'' \tag{3.49}$$

for class 2 events.

3.1.6.3 Lifetimes from first principles

It can be shown [46] that there is a relation between the imaginary part of the self energy Γ and the lifetimes through

$$\tau_\lambda = \frac{1}{2\Gamma_\lambda(\omega_\lambda)} \tag{3.50}$$

where Γ is

$$\Gamma_\lambda(\omega) = \frac{18\pi}{\hbar^2} \sum_{\lambda'\lambda''} |\Phi_{-\lambda\lambda'\lambda''}|^2 \Big\{ (n_{\lambda'} + n_{\lambda''} + 1)\, \delta(\omega - \omega_{\lambda'} - \omega_{\lambda''}) + (n_{\lambda'} - n_{\lambda''}) \big(\delta(\omega + \omega_{\lambda'} - \omega_{\lambda''}) - \delta(\omega - \omega_{\lambda'} + \omega_{\lambda''}) \big) \Big\}. \tag{3.51}$$

The constants $\Phi_{-\lambda\lambda'\lambda''}$ are the Fourier transforms of the third order IFCs after a transformation to normal modes. This expression can be obtained with a version of Fermi's golden rule. The golden rule states that the rate from an in-state $|\phi_{in}\rangle$ to an out-state $|\phi_{out}\rangle$ due to a perturbation H' is obtained by evaluating

$$P_{in\to out} = \frac{2\pi}{\hbar} |\langle \phi_{out}|H'|\phi_{in}\rangle|^2 \delta(E_{out} - E_{in}). \tag{3.52}$$

The delta function assures that the energy is conserved in the process. Besides that, the Fourier transform of the IFCs contains a factor that is non-zero only in the case that the crystal momenta is conserved up to a reciprocal vector.

The problem then comes down to calculating the third order IFCs. In this thesis a direct approach has been taken. The constants can be directly calculated by using finite differences on force data obtained from an electron structure calculation (see Sect. 3.3). All the IFCs can be obtained by calculating the forces in structures obtained by displacing one atom for the second order IFCs, and two atoms for the third order IFCs [47, 48]. For efficiency the symmetry of the system should be used to single out an irreducible set of displacements needed for a complete description of the forces in the material.

3.2 Molecular dynamics simulations

The Boltzmann equation has some problems handling effects that deviate from bulk homogeneous effects, for instance interfaces. One alternative approach that can handle these difficulties is molecular dynamics (MD) [49].

MD is in general an entirely classical method where, assuming the atomic force fields are known, integration of Newtons equation for a collection of interacting atoms is performed. One illuminating example of the MD method is the use of Verlet integration [50] to Newtons equations. Given interatomic forces $\boldsymbol{F}$ acting on an atom, Newton's equation of motion for that atom are

$$\boldsymbol{F} = m\boldsymbol{a}, \tag{3.53}$$

where m is the mass of the atom and $\boldsymbol{a}$ its acceleration. To integrate Eq. (3.53) one approach is to Taylor expand the position $\boldsymbol{r}$ around some time t giving

$$\begin{aligned} \boldsymbol{r}(t+\Delta t) &= \boldsymbol{r}(t) + \boldsymbol{v}(t)\Delta t + \frac{1}{2}\boldsymbol{a}(t)\Delta t^2 + \frac{1}{6}\boldsymbol{j}(t)\Delta t^3 + \mathcal{O}(\Delta t^4), \\ \boldsymbol{r}(t-\Delta t) &= \boldsymbol{r}(t) - \boldsymbol{v}(t)\Delta t + \frac{1}{2}\boldsymbol{a}(t)\Delta t^2 - \frac{1}{6}\boldsymbol{j}(t)\Delta t^3 + \mathcal{O}(\Delta t^4), \end{aligned} \tag{3.54}$$

where $\boldsymbol{j}$ is the jerk. Addition gives the Verlet integration as

$$\boldsymbol{r}(t+\Delta t) = 2\boldsymbol{r}(t) - \boldsymbol{r}(t-\Delta t) + \boldsymbol{a}(t)\Delta t^2 + \mathcal{O}(\Delta t^4). \tag{3.55}$$

This integration scheme is accurate to fourth order in time, velocity independent and only requires knowledge of the positions in the current as well as the last time step. Starting from two initial steps it is then possible to evolve the system in accordance with Newton's laws of motion.

Two limitations of MD can be mentioned. First, MD is a completely classical method and as such the average energy per phonon mode is $k_B T$ and can differ quite a bit from the true energy [51] see Eq. (3.26). Secondly, the number of atoms that need to be included can be quite high. To capture the behavior of a phonon the simulation domain should be at least twice as large as the respective phonon mean free path. Since the mean free path can be on the order of tens to hundreds of nanometers the number of atoms in the simulation may become intractable [51].

For MD simulations aiming at calculating the thermal conductivity there are two main approaches, the Green-Kubo method and the "direct method" [52] in the form of non-equilibrium molecular dynamics (NEMD).

The Green-Kubo method is an equilibrium approach where the equilibrium fluctuations are used to determine the lattice thermal conductivity through the Green-Kubo relations [53, 54, 55]. The Green-Kubo method exhibits slower convergence than than NEMD and thus requires more time steps [56]. It has also been demonstrated that there generally is an inconsistency between the results of the two methods in the case of conductance at the interface between two crystals [57].

The direct method, NEMD is much more straight forward. Typically, a simulation domain is set up with one hot region and cold region some distance apart. The outer regions are then connected through a periodic boundary. By fixing the

temperature in the hot region a temperature gradient can be established between the hot and the cold region by the use of an appropriate thermostat or swapping method. When a steady state has established and if the simulation has been properly done, the thermal conductivity can be determined with the use of Fourier's law.

3.3 Atomic forces from first principles

> That part there's just a joke. It's a spoof of the Born-Oppenheimer approximation.
>
> Sheldon Cooper

The IFCs introduced in Sect. 3.1.6 are calculated from knowledge of the forces between interacting atoms. In the present thesis, these forces were computed using quantum mechanical calculations.

The wave function of a quantum mechanical system $|\Psi\rangle$ is governed by the *Schrödinger equation* [58, 59]

$$i\hbar\frac{\partial\,|\Psi(t)\rangle}{\partial t} = H\,|\Psi(t)\rangle\,, \tag{3.56}$$

where the Hamiltonian H describes both internal and external interactions. The eigenspace of H is given as the solution to the eigenvalue problem

$$H\,|\psi\rangle = E\,|\psi\rangle\,. \tag{3.57}$$

The eigenvalues E are by *definition* the possible energies in a quantum mechanical system and thus solving Eq. (3.57) has merits of its own. The vectors $|\psi\rangle$ form a suitable basis for expanding the system $|\Psi\rangle$ and are the building blocks if one wants to construct a solution to Eq. (3.56).

In general, solving the Schrödinger equation directly is an impossible task, just as solving the Liouville equation, Eq. (3.4). The reason being that the quantum mechanical state is multidimensional in nature. This is a result [60] of the indistinguishable nature of quantum particles and the probabilistic interpretation of quantum states in accordance with the Born rule [61].

In matter the Hamiltonian can generally be written [62]

$$\begin{aligned} H = &-\frac{\hbar}{2m_e}\sum_i \nabla_i^2 - \frac{\hbar}{2M_I}\sum_I \nabla_I^2 \\ &+\frac{1}{2}\frac{1}{4\pi\epsilon_0}\sum_{i\neq j}\frac{e^2}{|\boldsymbol{r}_i-\boldsymbol{r}_j|} - \frac{1}{4\pi\epsilon_0}\sum_{i,I}\frac{Z_I e^2}{|\boldsymbol{r}_i-\boldsymbol{R}_I|} - \frac{1}{4\pi\epsilon_0}\sum_{I,J}\frac{Z_I Z_J e^2}{|\boldsymbol{R}_I-\boldsymbol{R}_J|}, \end{aligned} \tag{3.58}$$

where M_I and Z_I are the mass and charge of a nuclei, m_e the mass of an electron, e the fundamental charge and ϵ_0 the permittivity of free space. The position vectors $\boldsymbol{r}_i$ and $\boldsymbol{R}_I$ are with respect to an electron respectively a nuclei. The first two sums are operators for the kinetic energy of the electrons and the nuclei. The third sum comprises operators for the Coulomb interaction between electrons. The fourth sum contains interactions between electrons and the nuclei and the fifth, interactions between the nuclei.

The motion of the electrons and the nuclei are usually on such different timescale that the electronic part of the wave function can be separated from the part concerning the nuclei. Then the nuclei can be seen as frozen from the point of the electrons. This allows for a treatment where the electrons are viewed separately from the nuclei as an external potential, here noted V_{ext}. The Hamiltonian can now be written as [3]

$$h = -\frac{1}{2}\sum_i \nabla_i^2 + \frac{1}{2}\sum_{i\neq j}\frac{1}{|\boldsymbol{r}_i - \boldsymbol{r}_j|} + V_{ext}. \tag{3.59}$$

When the Schrödinger equation is solved for this system the force on the nuclei can be calculated with the Hellmann-Feynman force theorem [63]. With a solution for the ground-state energy E the theorem states that the force on ion I is given by

$$\boldsymbol{F}_I = -\frac{\partial E}{\partial \boldsymbol{R}_I}. \tag{3.60}$$

Still there is a problem. The Hamiltonian in h generates a problem with many degrees of freedom albeit the great simplification from the Born-Oppenheimer approximation. Also because of the term describing electron interaction the wave function is not separable into one-electron wave functions. There is thus still a need for further simplifications of the electronic structure problem defined by h.

3.4 Density functional theory

Density functional theory (DFT) nowadays refers to a collection of first-principals techniques using the electron density as a fundamental variable. The electron density in a system of electrons is defined as the number density of electrons in a specific state [64]. Suppressing spin the electron density is derived from the many-body electron wave function $|\Psi\rangle$ as

$$\rho(\boldsymbol{r}_1) = N\int d\boldsymbol{r}_2 \ldots \boldsymbol{r}_N \left|\Psi\right|^2. \tag{3.61}$$

[3] From here on Hartree units will be used. Then action is then measured in units of the reduced Planck constant, charge in units of the fundamental charge and mass in units of electron masses. Finally the vacuum permittivity is set to $1/4\pi$.

If possible, the electron density is a much leaner object to work with, compared to the multidimensional wave function.

Fortunately, Hohenberg and Kohn showed in 1964 [65] that the electron density can be considered as a fundamental property of the ground state in that the ground state wave function can be expressed as a functional of the electron density $\rho_0(\boldsymbol{r})$. Hence the ground state energy may be expressed as

$$E_0 = \langle \Psi[\rho_0(\boldsymbol{r})] \big| h \big| \Psi[\rho_0(\boldsymbol{r})] \rangle. \tag{3.62}$$

They also showed that there exist a general functional $F[\rho]$ expressing the energy contribution from the kinetic energy as well as the interaction among the electrons. Together with a part giving the interaction energy from electronic interaction with the external potential V_{ext}, the energy can be expressed as

$$E[\rho(\boldsymbol{r})] = F[\rho(\boldsymbol{r})] + \int d\boldsymbol{r}\, \rho(\boldsymbol{r}) V_{ext}(\boldsymbol{r}). \tag{3.63}$$

This energy is minimized by the ground state density. Unfortunately the functional is not known in general. The theorem shows its existence but gives no prescription on how to find F. Since the functional contains many-body effects that are not known it is not possible to use this formulation, that is F directly [66].

3.4.1 The Kohn-Sham ansatz

In 1965 Kohn and Sham [67] proposed an ansatz where the system of interacting electrons is recast into a system of non-interacting electrons, a much simpler problem than the original many-body problem. The main assumption is that if one can formulate an auxiliary problem, with the same ground state solution as in the full many-body problem, then a solution to the auxiliary system also solves the original problem. In the Kohn-Sham ansatz the functional $F[\rho(\boldsymbol{r})]$ in Eq. (3.63) is separated as

$$F[\rho(\boldsymbol{r})] = T_s[\rho(\boldsymbol{r})] + E_H[\rho(\boldsymbol{r})] + E_{xc}[\rho(\boldsymbol{r})]. \tag{3.64}$$

Here $T_s[\rho(\boldsymbol{r})]$ is the kinetic energy for non-interacting electrons and $E_H[\rho(\boldsymbol{r})]$ is the Hartee energy expressed as

$$E_H[\rho(\boldsymbol{r})] = \frac{1}{2} \int d\boldsymbol{r} d\boldsymbol{r}' \, \frac{\rho(\boldsymbol{r})\rho(\boldsymbol{r}')}{|\boldsymbol{r} - \boldsymbol{r}'|}. \tag{3.65}$$

Both of these terms are known. The unknown part $E_{xc}[\rho(\boldsymbol{r})]$ collects the more complicated many-body effects that are usually referred to as exchange and correlation.

In practice an effective potential is formulated as

$$V_{eff} = V_{ext} + V_H + V_{xc} \tag{3.66}$$

where V_H is the Hartree potential

$$V_H(\boldsymbol{r}) = \int d\boldsymbol{r}' \frac{\rho(\boldsymbol{r}')}{|\boldsymbol{r} - \boldsymbol{r}'|} \tag{3.67}$$

while the potential for exchange-correlation V_{xc} is the functional derivative of the exchange-correlation energy

$$V_{xc} = \frac{\delta E_{xc}[\rho(\boldsymbol{r})]}{\delta \rho(\boldsymbol{r})}. \tag{3.68}$$

The independence of the electrons allows for separation into single electron equations

$$\left(-\frac{1}{2}\nabla^2 + V_{eff}(\boldsymbol{r})\right)\psi_i(\boldsymbol{r}) = \varepsilon_i \psi_i(\boldsymbol{r}). \tag{3.69}$$

The Kohn-Sham orbitals $\psi_i(\boldsymbol{r})$ are under the constraint that

$$\rho(\boldsymbol{r}) = \sum_i f_i |\psi_i|^2, \tag{3.70}$$

where f_i is an occupation factor for electron state ψ_i. The formulation is exact although the functional for the exchange-correlation energy, $E_{xc}[\rho(\boldsymbol{r})]$ is unknown. Besides that there has been a great reduction in complexity from a quantum many-body problem into separate problems for independent electrons.

3.4.2 Exchange-correlation functionals

The unknown exchange-correlation functionals are in general complicated and approximations are necessary. The approximation presented in the original Kohn and Sham paper [67] assumes that the electron density in a local region is the same as the density in a uniform electron gas of density $\rho(\boldsymbol{r})$. The exchange-correlation energy is then given by

$$E_{xc}^{LDA}[\rho(\boldsymbol{r})] = \int d\boldsymbol{r}\ \rho(\boldsymbol{r})\varepsilon_{xc}^{LDA}[\rho(\boldsymbol{r})] \tag{3.71}$$

where the exchange-correlation energy for the uniform gas has a known solution [62]. The approximation is relatively simple considering the full problem, but has nonetheless proven itself in many applications over the years.

The LDA assumes a slowly varying electron density, so a natural step is to include effects of local variations in the exchange-correlation functional. This approach is the semi-local *generalized gradient approximation* (GGA). Here the exchange-correlation energy is assumed to be dependent on the electron density as well as the gradient of the density

$$E_{xc}^{GGA}[\rho(\boldsymbol{r}] = \int d\boldsymbol{r}\, \rho(\boldsymbol{r})\varepsilon_{xc}^{GGA}[\rho(\boldsymbol{r}), \nabla\rho(\boldsymbol{r})]. \tag{3.72}$$

There are many versions of GGAs. Most notable is the PBE functional [68], which has been successfully used in many applications.

3.4.3 van der Waals density functionals

The van der Waals force is the result of non-local correlation between electrons. Because of the non-local nature of the van der Waals force, it is not expected that a local or semi-local approximation will give a correct exchange-correlation energy.

In Papers I and II, first-principles calculations were conducted on van der Waals solids [69]. To describe van der Waals solids properly within DFT it is important to use a proper a van der Waals density functional (vdW-DF) that captures the sparse nature [70] of the materials. In 2003 a vdW-DF addressing layered structures [71] was presented, followed one year later by a vdW-DF for general structures [72].

In the vdW-DF method the correlation energy assumes a non-local form, which is expressed as a double integral over the spatial degrees of freedom [73]

$$E_c^{\mathrm{nl}}[\rho] = \frac{1}{2}\int\int \rho(\boldsymbol{r})\phi(\boldsymbol{r},\boldsymbol{r}')\rho(\boldsymbol{r}')d^3\boldsymbol{r}d^3\boldsymbol{r}', \tag{3.73}$$

where the kernel $\phi(\boldsymbol{r},\boldsymbol{r}')$ represents the non-local coupling of the electron densities at $\boldsymbol{r}$ and $\boldsymbol{r}'$. The correlation energy is usually complemented by a semi-local exchange functional,

$$E_{xc}^{vdW-DF}[\rho(\boldsymbol{r})] = E_x^{sl}[\rho(\boldsymbol{r})] + E_c^{nl}[\rho(\boldsymbol{r})], \tag{3.74}$$

which historically was adapted from other semi-local exchange-correlation functionals. In 2014 a consistent exchange (CX) part was developed leading to the so-called vdW-DF-CX functional [74], which was used in Papers I and II of the present thesis.

3.4.4 Fourier expansion and pseudopotentials

In a solid, periodic boundary conditions are suitable for calculating bulk properties where surface effects are negligible. This is reasonable if the considered system is

large compared to the boundaries. Effectively, by introducing periodic boundaries the computational system becomes infinite. In the case of a wave function, due to the theorem by Bloch [75] it is possible to expand the wave function in a plane wave basis set that is complete as long as the wave vectors in the first Brillouin zone are included. This is done by Fourier expansion over the reciprocal lattice vectors $\boldsymbol{G}$ through the series

$$\psi_{n,\boldsymbol{k}}(\boldsymbol{r}) = \sum_{\boldsymbol{G}} c_{n,\boldsymbol{k}+\boldsymbol{G}} \exp\left[i(\boldsymbol{k}+\boldsymbol{G})\cdot\boldsymbol{r}\right]. \tag{3.75}$$

This sum is infinite and for practical purposes the series must be truncated by a cutoff. The Fourier coefficients $c_{n,\boldsymbol{k}+\boldsymbol{G}}$ decrease for increasing $\left|\boldsymbol{k}+\boldsymbol{G}\right|$ [66]. So introduction of an energy cutoff E_{cut} allows for expansion including only the reciprocal vectors that fulfill the condition

$$\frac{\hbar^2}{2m}\left|\boldsymbol{k}+\boldsymbol{G}\right|^2 < E_{cut}. \tag{3.76}$$

With an increasing number of nodes, a wave function picks up an oscillating behavior near the nuclei [76]. Oscillations are more complicated to handle computationally and cause slow convergence[4]. Since core electrons are not strongly involved in interaction with valence electrons, for the sake of chemical bonding, it is not necessary to have a detailed description of the wave functions close to the nuclei. To overcome this issue one frequently employs so-called pseudopotentials, which replace the full Coulomb potential corresponding to the ionic core with a smoother potential that incorporates the core electrons and has the same scattering properties as the original potential [62]. Common schemes include norm-conserving and ultra-soft pseudopotentials [77]. In the present work the project augmented wave (PAW)[78] method was employed, which represents a bridge between pseudopotential and all-electron type calculations.

[4]More coefficients are necessary in the Fourier expansion

4

Summary of the papers

4.1 Paper I: Ultra-low thermal conductivity in WSe_2

Tungsten diselenide (WSe_2) is a van der Waals (vdW) solid that consists of two-dimensional sheets with strong intralayer bonding and interplanar vdW coupling. Van der Waals solids have a highly anisotropic thermal conductivity with an out-of-plane conductivity $\kappa_\perp$ for bulk material of 1.5 W/mK at room temperature [79]. It was experimentally demonstrated that $\kappa_\perp$ in turbostratically deposited WSe_2 films can be reduced down to 0.05 W/mK. This is a factor of 30 lower than in bulk crystals and thus considerably below the conservative estimate of the minimum thermal conductivity thought achievable.

In this paper a microscopic model was developed to explain this observation of an ultra-low thermal conductivity in disordered thin films of WSe_2. This was accomplished within the framework of Boltzmann transport theory and the relaxation time approximation (Sect. 3.1.5) based on second order force constants calculated within density functional theory. To accurately capture nonlocal correlation effects a non-empirical consistent exchange vdW density functional (vdW-DF-CX) was used [74].

First the sensitivity of the lattice thermal conductivity to different planar defects was established. Stacking disorder and strain cause phonon localization and softening of the acoustic modes, which can account for a reduction of $\kappa_\perp$ by a factor of 2 to 4 (green dashed line in Fig. 4.1). In addition the layer disorder introduces a structural limit on the phonon mean free path, which can be reduced to the separation between individual layers. Assuming that this limitation can be modeled by a diffuse boundary scattering model reduces the conductivity as well (green band

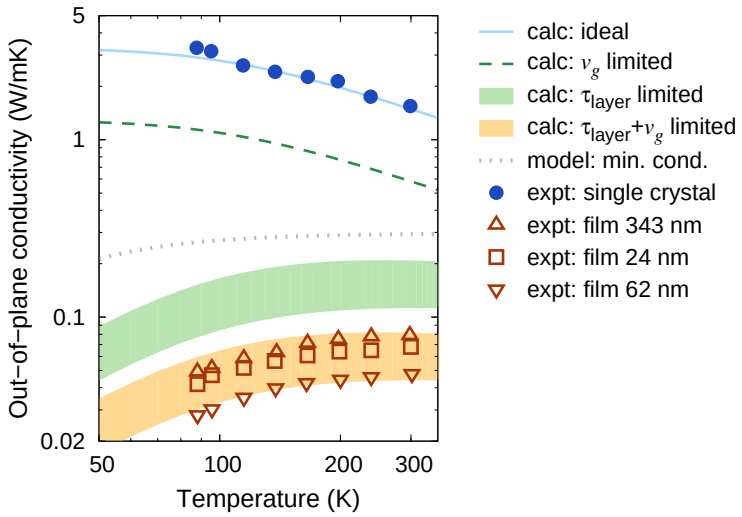

Figure 4.1: The experimentally measured reduced lattice thermal conductivity in disordered thin WSe_2 films corresponds to the red triangles and squares (Cahill et. al. [79]). The measured values in a single bulk crystal corresponds to the blue dots. Reduction of group velocities lowers the lattice thermal conductivity to the green dashed line. Lifetime reductions due to strong boundary scattering associated with disorder reduces the conductivity to the green band. Adding the effect of both group velocity reduction as well as lowered lifetime as a result of increased scattering reduces the predicted lattice thermal conductivity to the yellow band.

in Fig. 4.1). If the effect of group velocity and lifetime reduction are combined one obtains a lattice thermal conductivity that is comparable to the measured data (yellow band in Fig. 4.1).

The results show that a reduction of $\kappa_\perp$ by 40-60% can be achieved merely by variations in the layer stacking, which is associated with only a small energy cost. This can be important for e.g., thermoelectric applications where a low thermal conductivity in conjunction with a high electrical conductivity is necessary to achieve a high thermodynamic efficiency. Since electrons typically have larger mean free paths than phonons, they are less likely to be affected by changes in the stacking order, thus creating the possibility to decouple electrical and thermal transport properties. While the model was developed for WSe_2 it is likely to be also applicable to similar vdW solids.

4.2 Paper II: Thermal conductivity in van der Waals solids

Novel synthesis techniques [80, 81] provide the opportunity to create highly engineered van der Waals (vdW) solids, which emerge as promising candidates for a manifold of applications including electronic components [18], optoelectronics [19, 20, 21], thermoelectrics [22], and spintronics [23]. Since thermal transport plays a key role in many of these situations, it is important to develop a detailed understanding of the thermal conductivity κ in vdW solids.

Unfortunately, values for the thermal conductivities reported in the literature exhibit a wide spread and can differ by more than one order of magnitude. This can be partly attributed to the challenges associated with experimental measurements of the thermal conductivity in nanostructures with pronounced anisotropy, see e.g., [82, 83]. Possibly even more crucial is the sensitivity of the results to defects and sample size effects, as the growth of large high-quality TMD single crystals is very time consuming [83].

Given this motivation the present paper investigates the finite temperature properties as well as the lattice thermal conductivity κ in Mo and W-based transition metal dichalcogenides (TMDs) employing a combination of density functional and Boltzmann transport theory. Once again the calculations were carried out using the vdW-DF-CX functional, which is shown to yield excellent agreement with experimental lattice constants at room temperature with an average relative error below 0.2%.

With regard to the thermal conductivity it is demonstrated that care must be taken with regard to some computational parameters, in particular the displacement amplitude used for evaluating finite differences. A careful analysis shows that larger values than commonly used for e.g., materials such as silicon, are required in order to balance numerical accuracy with the smallness of vdW forces.

The calculated in-plane conductivities at room temperature are in good agreement with experimental data for high-purity material, when only phonon-phonon and isotopic scattering are included. Explaining the experimental data over the entire temperature, however, requires inclusion of a temperature independent scattering mechanism that limits the phonon mean free path (MFP). The latter effect is even more pronounced in the case of the out-of-plane conductivity.

The sensitivity of the thermal conductivity to structural inhomogeneities can be rationalized in terms of the long MFPs of the modes that contribute the most strongly to κ. The MFP of these modes (including phonon-phonon and isotopic scattering) is at least 1 μm, which is comparable to silicon but much larger than e.g., PbTe. This behavior is promising for thermoelectric applications, where lowering the lattice part of the thermal conductivity is a widely employed approach for in-

creasing the thermodynamic efficiency. On the other hand, it can pose problems for electronic and optoelectronic applications, which require a large κ for rapid heat dissipation.

Overall the present study provides a comprehensive set of lattice thermal conductivities for bulk TMDs that establishes bounds set by phonon-phonon scattering and intrinsic length scales. It thereby forms the basis for future studies on these systems, which could focus e.g., on genuine vdW solids comprising different layers.

4.3 Paper III: Thermal conductivity in clathrates

Clathrates are chemical substances with a defined lattice structure that can trap atomic or molecular species [24, 25]. Inorganic clathrates such as $Ba_8Ga_{16}Ge_{30}$ or $Sr_8Ga_{16}Sn_{30}$ exhibit a combination of electrical and thermal transport properties that is very favorable for thermoelectric applications [26, 27]. Here, the earth alkaline atoms act as guest species that occupy the cages provided by the host structure, which is most commonly composed of elements from groups 13 and 14. Since the guest atoms in these structures can exhibit "rattler"-like atomic motion due to their relatively small size compared to the available cage [28, 29, 30], they have been linked to the very small lattice thermal conductivity κ_l [31, 32].

In this paper, the electrical and thermal transport properties of $Ba_8Ga_{16}Ge_{30}$ where studied as a function of the chemical order. Using alloy cluster expansions trained by density functional theory calculations the chemical order in the form of the site occupancy factors was determined as a function of temperature. In this fashion the chemically ordered ground state was determined, which subsequently served as a starting point for further studies.

The author's contribution concerned the calculation and analysis of the lattice thermal conductivity of $Ba_8Ga_{16}Ge_{30}$, which was achieved within the framework of Boltzmann transport theory based on the calculation of both second and third order force constants from first principles. The thermal conductivity unlike the electrical transport coefficients is shown to be rather insensitive to the chemical order. When phonon-phonon and isotope scattering are taken into account, the calculations are in reasonable agreement with experiment, albeit somewhat too low. A closer inspection of the results reveals that only modes with frequencies below 0.5 THz make a substantial contribution to the room temperature conductivity. Modes above this cutoff, the frequencies of which extend up to 8 THz, have extremely short lifetimes, which outweigh the rather large group velocities of at least some of these phonons. The extremely small lattice conductivity is thus primarily the result of the very small Brillouin zone volume occupied by phonon modes available for thermal transport.

5

Outlook

In the present thesis two different types of materials were investigated with regard to their ability to transport heat. Papers I and II addressed layered materials with very anisotropic properties. Because of the weak interlayer binding they are prone to form planar defects, which as shown in this thesis can have dramatic effects on their ability to conduct heat. At the same time, the 2D character of the individual sheets enables the fabrication of heterostructures composed of layers of different 2D materials including but not limited to the transition metal dichalcogenides (TMDs) investigated in the present thesis. Thus while in the present thesis the focus has been on homogeneous materials, in the future this research ought to be extended to heterostructures composed of different TMDs and not necessarily limited to Mo and W-based compounds.

It was discussed in Paper II how differences in mass and structure affect the phonon dispersion, which in turn determines to a large extent the lattice thermal conductivity. By combining different layers it becomes possible to engineer these features and to manipulate both out-of-plane and in-plane transport in a very controlled fashion. In this context, the approach taken in Paper III is potentially very powerful, i.e. by combining transport calculations with effective models (such as the cluster expansions in Paper III) and sampling techniques (e.g., Monte Carlo simulations or genetic algorithms) one can computationally design structures with specified transport properties. This "inverse design" approach was adopted in Paper III to optimize electrical transport properties in clathrates but is in principle equally applicable to thermal transport. Conversely, it will be interesting to explore electrical transport in van der Waals solids and specifically to explore strategies for controlling electron-phonon coupling and decoupling electronic and thermal transport.

The insight and results gained in this thesis are not only important for our un-

derstanding of van der Waals solids and thermoelectric materials but for thermal transport in general. In the future, the goal will be to implement the concepts developed here in experimental settings and to push the limits of materials and transport. In this fashion this thesis will ultimately contribute to the vast and important field of energy management.

A

Liouville's theorem

The following short section gives a derivation of *Liouville's theorem*. This theorem is of importances in the theoretical framework of a statistical treatment of transport phenomena [84] and the foundation on which the *Boltzmann equation* is formally derived.

Start by introducing a compact notation for the $6N$ generalized coordinates and momenta in phase space as $q = q_1, \dots, q_{3N}$ and $p = p_1, \dots, p_{3N}$. Let the corresponding volume element be $dqdp = dq_1 \cdots dq_{3N} dp_1 \cdots dp_{3N}$. Let $\rho(q, p, t)$ be the number density of states in phases space so that

$$\rho(q, p, t)\, dqdp \tag{A.1}$$

corresponds to the number of states in the volume element at time t. Let V be a constant volume in phase space and S the surface that enclose V. The rate of change in the number of states in V is then

$$\frac{\partial}{\partial t} \int_V \rho\, dqdp. \tag{A.2}$$

As long as no states are produced or destroyed within V the rate at wich the number of states changes must equal the net transport of states over S

$$\frac{\partial}{\partial t} \int_V \rho\ dqdp = -\int_S \rho\, \boldsymbol{v} \cdot \boldsymbol{n}\, dS. \tag{A.3}$$

Here $\boldsymbol{v}$ is the velocity field [1] across the surface and $\boldsymbol{n}$ the outbound normal. Using

[1] A velocity field in the generalized sense that

$$\boldsymbol{v} = \Big(\frac{\partial q_1}{\partial t}, \dots, \frac{\partial q_{3N}}{\partial t}, \frac{\partial q_1}{\partial t}, \dots, \frac{\partial p_{3N}}{\partial t} \Big).$$

the divergence theorem the surface integral can be changed into a volume integral over the divergence of $\rho \boldsymbol{v}$. Since the control volume is not changing the time derivative can be taken inside the volume integral over ρ and a re-arrangement gives

$$\int_V \Big(\frac{\partial \rho}{\partial t} + \nabla \cdot (\rho \boldsymbol{v}) \Big) dV = 0. \tag{A.4}$$

The volume is arbitrarily chosen so the integrand must vanish identically. Hence

$$\frac{\partial \rho}{\partial t} + \nabla \cdot (\rho \boldsymbol{v}) = 0. \tag{A.5}$$

Applying the product rule on the terms in the expanded divergence in the continuity equation equals

$$\frac{\partial \rho}{\partial t} + \sum_{i=1}^{3N} \Big(\frac{\partial \rho}{\partial q_i} \frac{\partial q_i}{\partial t} + \frac{\partial \rho}{\partial p_i} \frac{\partial p_i}{\partial t} \Big) + \rho \sum_{i}^{3N} \Big(\frac{\partial^2 q_i}{\partial q_i \partial t} + \frac{\partial^2 p_i}{\partial p_i \partial t} \Big) = 0. \tag{A.6}$$

For each pair of conjugate variables the canonical equations read [85]

$$\begin{aligned} \frac{\partial q_i}{\partial t} &= \quad \frac{\partial H}{\partial p_i} \\ \frac{\partial p_i}{\partial t} &= -\frac{\partial H}{\partial q_i}, \end{aligned} \tag{A.7}$$

where $H(q, p)$ is the Hamiltonian, and so each term in the last sum in Eq. (A.6) is identically zero since partial derivatives commute. Due to the chain rule combined with the Poisson bracket [2] the remaining part of the continuity equation can now be written as the total derivative

$$\begin{aligned} \frac{d\rho}{dt} &= \frac{\partial \rho}{\partial t} + \sum_{i=1}^{3N} \Big(\frac{\partial \rho}{\partial q_i} \frac{\partial q_i}{\partial t} + \frac{\partial \rho}{\partial p_i} \frac{\partial p_i}{\partial t} \Big) \\ &= \frac{\partial \rho}{\partial t} + \sum_{i=1}^{3N} \Big(\frac{\partial \rho}{\partial q_i} \frac{\partial H}{\partial p_i} - \frac{\partial \rho}{\partial p_i} \frac{\partial H}{\partial q_i} \Big) \\ &= \frac{\partial \rho}{\partial t} + \big\{ \rho, H \big\} = 0. \end{aligned} \tag{A.8}$$

[2] The Poisson bracket for a quantity A related to a dynamical system governed by the Hamiltonian H is defined as

$$\big\{ A, H \big\} = \sum_{i=1}^{3N} \Big(\frac{\partial A}{\partial q_i} \frac{\partial H}{\partial p_i} - \frac{\partial A}{\partial p_i} \frac{\partial H}{\partial q_i} \Big).$$

This resembles the result for an incompressibel fluid and one can think of the number densities of states in phase space as constituting an incompressible fluid. In the fixed frame of reference it is then shown that the total derivative of the number density function is zero. In the opposite frame, the co-moving frame that follows the fluid motion the number density doesn't change with time. This has the implication that a volume element in phase-space is invariant over time. This is the result known as *Liouville's theorem* and equation Eq. (A.8) is called *Liouville's equation*.

Acknowledgments

My deepest and sincerest gratitude goes to my main supervisor *Paul Erhart*. His enthusiasm and dedication is more than any student could wish for.

Many thanks to everyone in the group, you all make it even easier to work here.

There is also a person outside our little group that deserves some attention. *Adam* consider yourself acknowledged.

And at last, this thesis is dedicated to my wife Hanna and our daughters Nova and Lilo. Thank you for your support, I love you with all my heart.

Bibliography

[1] M. Kardar, *Statistical Physics of Particles*, 1 edition ed. (Cambridge University Press, Cambridge : New York, 2007).

[2] International Energy Agency, *Key World Energy Statistics 2015*, http://www.iea.org, 2015, accessed: 2016-05-14.

[3] R. Bookstaber, *A Demon of Our Own Design: Markets, Hedge Funds, and the Perils of Financial Innovation* (Wiley, Hoboken, N. J., 2008).

[4] United Nations - Department of Economic and Social Affairs, http://esa.un.org/unpd/wpp/Download/Standard/Population/, data accessed: 2016-05-14.

[5] H. D. Klemme and G. F. Ulmishek, *Effective Petroleum Source Rocks of the World: Stratigraphic Distribution and Controlling Depositional Factors (1)*, AAPG Bulletin **75**, 1809 (1991).

[6] G. Bowden, *The Social Construction of Validity in Estimates of US Crude Oil Reserves*, Social Studies of Science **15**, 207 (1985).

[7] K. Aleklett, M. Lardelli, and O. Qvennerstedt, *Peeking at peak oil* (Springer, New York ; London, 2012).

[8] K. Aleklett, M. Höök, K. Jakobsson, M. Lardelli, S. Snowden, and B. Söderbergh, *The Peak of the Oil Age – Analyzing the world oil production Reference Scenario in World Energy Outlook 2008*, Energy Policy **38**, 1398 (2008).

[9] I. Chapman, *The end of Peak Oil? Why this topic is still relevant despite recent denials*, Energy Policy **64**, 93 (2014).

[10] U. S. Energy Information Agency, *International Energy Statistics - Total Primary Energy Production*, http://www.eia.gov/cfapps/ipdbproject/IEDIndex3.cfm, data accessed: 2016-05-14.

[11] Intergovernmental Panel on Climate Change, *Climate Change 2013 - The Physical Science Basis: Working Group I Contribution to the Fifth Assessment Report of the Intergovernmental Panel on Climate Change*, 1 edition ed. (Cambridge University Press, New York, 2014).

[12] Y. Demirel, *Energy: production, conversion, storage, conservation, and coupling*, *Green energy and technology* (Springer, London ; New York, 2012).

[13] H. B. Callen, *Thermodynamics and an introduction to thermostatistics* (Wiley, New York, 1985).

[14] S. R. D. Groot and P. Mazur, *Non-Equilibrium Thermodynamics*, dover ed edition ed. (Dover Publications, New York, 2011).

[15] *CRC Handbook of Thermoelectrics*, 1 edition ed., edited by D. M. Rowe (CRC Press, Boca Raton, FL, 1995).

[16] D. M. Rowe, *Thermoelectrics handbook: macro to nano-structured materials* (CRC Press, Boca Raton, FL, 2005).

[17] J. M. Ziman, *Electrons and phonons* (Clarendon Press, Oxford, 1960).

[18] B. Radisavljevic, A. Radenovic, J. Brivio, V. Giacometti, and A. Kis, *Single-layer MoS_2 transistors*, Nature Nanotech. **6**, 147 (2011).

[19] Q. H. Wang, K. Kalantar-Zadeh, A. Kis, J. N. Coleman, and M. S. Strano, *Electronics and optoelectronics of two-dimensional transition metal dichalcogenides*, Nature Nanotech. **7**, 699 (2012).

[20] X. Hong, J. Kim, S.-F. Shi, Y. Zhang, C. Jin, Y. Sun, S. Tongay, J. Wu, Y. Zhang, and F. Wang, *Ultrafast charge transfer in atomically thin MoS_2/WS_2 heterostructures*, Nature Nanotech. **9**, 682 (2014).

[21] M. Massicotte, P. Schmidt, F. Vialla, K. G. Schädler, A. Reserbat-Plantey, K. Watanabe, T. Taniguchi, K. J. Tielrooij, and F. H. L. Koppens, *Picosecond photoresponse in van der Waals heterostructures*, Nature Nanotech. **11**, 42 (2016).

[22] H. Guo, T. Yang, P. Tao, Y. Wang, and Z. Zhang, *High pressure effect on structure, electronic structure, and thermoelectric properties of MoS_2*, J. Appl. Phys. **113**, 013709 (2013).

[23] W. Han, *Perspectives for spintronics in 2D materials*, APL Materials **4**, 032401 (2016).

[24] A. D. McNaught and A. Wilkinson, *IUPAC. Compendium of Chemical Terminology*, 2nd ed. (Blackwell Scientific Publications, Oxford, 1997), XML online corrected version: http://goldbook.iupac.org (2006-) created by M. Nic, J. Jirat, B. Kosata; updates compiled by A. Jenkins.

[25] G. P. Moss, P. A. S. Smith, and D. Tavernier, *Glossary of class names of organic compounds and reactivity intermediates based on structure (IUPAC Recommendations 1995)*, Pure and Applied Chemistry **67**, 1307 (2009).

[26] P. Rogl, *Thermoelectrics Handbook* (CRC Press, Boca Raton, 2005), Chap. 32, pp. 1–24.

[27] A. V. Shevelkov and K. Kovnir, in *Zintl Phases*, No. 139 in *Structure and Bonding*, edited by T. F. Fässler (Springer, Berlin, Heidelberg, 2011), pp. 97–142.

[28] G. K. H. Madsen and G. Santi, *Anharmonic lattice dynamics in type-I clathrates from first-principles calculations*, Phys. Rev. B **72**, 220301 (2005).

[29] M. Christensen, A. B. Abrahamsen, N. B. Christensen, F. Juranyi, N. H. Andersen, K. Lefmann, J. Andreasson, C. R. H. Bahl, and B. B. Iversen, *Avoided crossing of rattler modes in thermoelectric materials*, Nature Mater. **7**, 811 (2008).

[30] Y. He and G. Galli, *Nanostructured Clathrate Phonon Glasses: Beyond the Rattling Concept*, Nano Lett. **14**, 2920 (2014).

[31] J. L. Cohn, G. S. Nolas, V. Fessatidis, T. H. Metcalf, and G. A. Slack, *Glasslike Heat Conduction in High-Mobility Crystalline Semiconductors*, Phys. Rev. Lett. **82**, 779 (1999).

[32] J. Dong, O. F. Sankey, and C. W. Myles, *Theoretical Study of the Lattice Thermal Conductivity in Ge Framework Semiconductors*, Phys. Rev. Lett. **86**, 2361 (2001).

[33] M. Christensen, S. Johnsen, and B. B. Iversen, *Thermoelectric clathrates of type I*, Dalton Trans. **39**, 978 (2010).

[34] B. C. Sales, B. C. Chakoumakos, R. Jin, J. R. Thompson, and D. Mandrus, *Structural, magnetic, thermal, and transport properties of $X_8Ga_{16}Ge_{30}$ (X=Eu, Sr, Ba) single crystals*, Phys. Rev. B **63**, 245113 (2001).

[35] J. D. Bryan, N. P. Blake, H. Metiu, G. D. Stucky, B. B. Iversen, R. D. Poulsen, and A. Bentien, *Nonstoichiometry and chemical purity effects in thermoelectric $Ba_8Ga_{16}Ge_{30}$ clathrate*, Journal of Applied Physics **92**, 7281 (2002).

[36] A. Saramat, G. Svensson, A. E. C. Palmqvist, C. Stiewe, E. Mueller, D. Platzek, S. G. K. Williams, D. M. Rowe, J. D. Bryan, and G. D. Stucky, *Large thermoelectric figure of merit at high temperature in Czochralski-grown clathrate $Ba_8Ga_{16}Ge_{30}$*, J. Appl. Phys. **99**, 023708 (2006).

[37] M. Christensen, N. Lock, J. Overgaard, and B. B. Iversen, *Crystal Structures of Thermoelectric n- and p-type $Ba_8Ga_{16}Ge_{30}$ Studied by Single Crystal, Multitemperature, Neutron Diffraction, Conventional X-ray Diffraction and Resonant Synchrotron X-ray Diffraction*, J. Am. Chem. Soc. **128**, 15657 (2006).

[38] E. S. Toberer, M. Christensen, B. B. Iversen, and G. J. Snyder, *High temperature thermoelectric efficiency in $Ba_8Ga_{16}Ge_{30}$*, Phys. Rev. B **77**, 075203 (2008).

[39] D. Cederkrantz, A. Saramat, G. J. Snyder, and A. E. C. Palmqvist, *Thermal stability and thermoelectric properties of p-type $Ba_8Ga_{16}Ge_{30}$ clathrates*, J. Appl. Phys. **106**, 074509 (2009).

[40] N. P. Blake, S. Latturner, J. D. Bryan, G. D. Stucky, and H. Metiu, *Band structures and thermoelectric properties of the clathrates $Ba_8Ga_{16}Ge_{30}$, $Sr_8Ga_{16}Ge_{30}$, $Ba_8Ga_{16}Si_{30}$, and $Ba_8In_{16}Sn_{30}$*, J. Chem. Phys. **115**, 8060 (2001).

[41] N. P. Blake, D. Bryan, S. Latturner, L. Mollnitz, G. D. Stucky, and H. Metiu, *Structure and stability of the clathrates $Ba_8Ga_{16}Ge_{30}$, $Sr_8Ga_{16}Ge_{30}$, $Ba_8Ga_{16}Si_{30}$, and $Ba_8In_{16}Sn_{30}$*, J. Chem. Phys. **114**, 10063 (2001).

[42] G. K. H. Madsen, K. Schwarz, P. Blaha, and D. J. Singh, *Electronic structure and transport in type-I and type-VIII clathrates containing strontium, barium, and europium*, Phys. Rev. B **68**, 125212 (2003).

[43] B. Eisenmann, H. Schäfer, and R. Zagler, *Die Verbindungen $A_8^{II}B_{16}^{III}B_{30}^{IV}$ (A^{II} = Sr, Ba; B^{III}= Al, Ga; B^{IV} = Si, Ge, Sn) und ihre Käfigstrukturen*, Journal of the Less Common Metals **118**, 43 (1986).

[44] H. Goldstein, *Classical Mechanics*, 2nd edition ed. (Addison-Wesley, Reading, Mass, 1980).

[45] J. J. Sakurai and S. F. Tuan, *Modern quantum mechanics*, rev. ed ed. (Addison-Wesley, Reading, Mass, 1994).

[46] G. P. Srivastava, *The physics of phonons* (Hilger, Bristol, 1990).

[47] W. Li, J. Carrete, N. A. Katcho, and N. Mingo, *ShengBTE: A solver of the Boltzmann transport equation for phonons*, Comp. Phys. Comm. **185**, 1747 (2014).

[48] A. Togo, L. Chaput, and I. Tanaka, *Distributions of phonon lifetimes in Brillouin zones*, Phys. Rev. B **91**, 094306 (2015).

[49] D. Frenkel and B. Smit, *Understanding Molecular Simulation* (Academic Press, London, 2001).

[50] L. Verlet, *Computer 'experiments' on classical fluids I. Thermodynamical properties of Lennard-Jones molecules*, Phys. Rev. **159**, 98 (1967).

[51] D. G. Cahill, P. V. Braun, G. Chen, D. R. Clarke, S. Fan, K. E. Goodson, P. Keblinski, W. P. King, G. D. Mahan, A. Majumdar, H. J. Maris, S. R. Phillpot, E. Pop, and L. Shi, *Nanoscale thermal transport. II. 2003–2012*, Applied Physics Reviews **1**, 011305 (2014).

[52] D. G. Cahill, W. K. Ford, K. E. Goodson, G. D. Mahan, A. Majumdar, H. J. Maris, R. Merlin, and S. R. Phillpot, *Nanoscale thermal transport*, J. Appl. Phys. **93**, 793 (2003).

[53] M. S. Green, *Markoff Random Processes and the Statistical Mechanics of Time-Dependent Phenomena. II. Irreversible Processes in Fluids*, The Journal of Chemical Physics **22**, 398 (1954).

[54] R. Kubo, M. Yokota, and S. Nakajima, *Statistical-Mechanical Theory of Irreversible Processes. II. Response to Thermal Disturbance*, Journal of the Physical Society of Japan **12**, 1203 (1957).

[55] M. Toda, R. Kubo, and N. Hashitsume, *Statistical physics. 2, Nonequilibrium statistical mechanics*, No. 31 in *Springer series in solid-state sciences*, 2. ed ed. (Springer, Berlin ; New York, 1991).

[56] P. K. Schelling, S. R. Phillpot, and P. Keblinski, *Comparison of atomic-level simulation methods for computing thermal conductivity*, Physical Review B **65**, 144306 (2002).

[57] S. Merabia and K. Termentzidis, *Thermal conductance at the interface between crystals using equilibrium and nonequilibrium molecular dynamics*, Phys. Rev. B **86**, 094303 (2012).

[58] E. Schrödinger, *An Undulatory Theory of the Mechanics of Atoms and Molecules*, Physical Review **28**, 1049 (1926).

[59] R. Shankar, *Principles of quantum mechanics*, 2. ed ed. (Plenum, New York, 1994).

[60] H. Kroemer, *Quantum Mechanics For Engineering: Materials Science and Applied Physics* (Pearson, Englewood Cliffs, N.J, 1994).

[61] M. Born, *Quantenmechanik der Stoßvorgänge*, Zeitschrift für Physik **38**, 803 (1926).

[62] R. M. Martin, *Electronic structure: basic theory and practical methods* (Cambridge Univ. Press, Cambridge, 2004).

[63] R. P. Feynman, *Forces in Molecules*, Physical Review **56**, 340 (1939).

[64] R. G. Parr and W. Yang, *Density-Functional Theory of Atoms and Molecules* (Oxford University Press, New York, 1989).

[65] P. Hohenberg and W. Kohn, *Inhomogeneous Electron Gas*, Phys. Rev. **136**, B864 (1964).

[66] P. J. Kohanoff, *Electronic Structure Calculations for Solids and Molecules: Theory and Computational Methods*, 1 edition ed. (Cambridge University Press, Cambridge, UK ; New York, 2006).

[67] W. Kohn and L. J. Sham, *Self-Consistent Equations Including Exchange and Correlation Effects*, Phys. Rev. **140**, A1133 (1965).

[68] J. P. Perdew, K. Burke, and M. Ernzerhof, *Generalized Gradient Approximation Made Simple*, Phys. Rev. Lett. **77**, 3865 (1996), erratum, *ibid.* **78**, 1396(E) (1997).

[69] G. Gao, W. Gao, E. Cannuccia, J. Taha-Tijerina, L. Balicas, A. Mathkar, T. N. Narayanan, Z. Liu, B. K. Gupta, J. Peng, Y. Yin, A. Rubio, and P. M. Ajayan, *Artificially Stacked Atomic Layers: Toward New van der Waals Solids*, Nano Lett. **12**, 3518 (2012).

[70] D. C. Langreth, B. I. Lundqvist, S. D. Chakarova-Käck, V. R. Cooper, M. Dion, P. Hyldgaard, A. Kelkkanen, J. Kleis, L. Kong, S. Li, P. G. Moses, E. Murray, A. Puzder, H. Rydberg, E. Schröder, and T. Thonhauser, *A density functional for sparse matter*, J. Phys. Condens. Matter **21**, 084203 (2009).

[71] H. Rydberg, M. Dion, N. Jacobson, E. Schröder, P. Hyldgaard, S. I. Simak, D. C. Langreth, and B. I. Lundqvist, *Van der Waals Density Functional for Layered Structures*, Phys. Rev. Lett. **91**, 126402 (2003).

[72] M. Dion, H. Rydberg, E. Schröder, D. C. Langreth, and B. I. Lundqvist, *Van der Waals Density Functional for General Geometries*, Phys. Rev. Lett. **92**, 246401 (2004).

[73] K. Berland, C. Arter, V. R. Cooper, K. Lee, B. I. Lundqvist, E. Schröder, T. Thonhauser, and P. Hyldgaard, *van der Waals density functionals built upon the electron-gas tradition: Facing the challenge of competing interactions*, J. Chem. Phys. **140**, 18A539 (2014).

[74] K. Berland and P. Hyldgaard, *Exchange functional that tests the robustness of the plasmon description of the van der Waals density functional*, Physical Review B **89**, 035412 (2014).

[75] F. Bloch, *Über die Quantenmechanik der Elektronen in Kristallgittern*, Zeitschrift für Physik **52**, 555 (1929).

[76] B. H. Bransden and C. J. Joachain, *Physics of atoms and molecules*, 2. ed ed. (Prentice Hall, Upper Saddle River, N.J, 2003).

[77] D. Vanderbilt, *Soft self-consistent pseudopotentials in a generalized eigenvalue formalism*, Phys. Rev. B **41**, 7892 (1990).

[78] P. E. Blöchl, *Projector augmented-wave method*, Phys. Rev. B **50**, 17953 (1994).

[79] C. Chiritescu, D. G. Cahill, N. Nguyen, D. Johnson, A. Bodapati, P. Keblinski, and P. Zschack, *Ultralow Thermal Conductivity in Disordered, Layered WSe_2 Crystals*, Science **315**, 351 (2007).

[80] A. K. Geim and I. V. Grigorieva, *Van der Waals heterostructures*, Nature **499**, 419 (2013).

[81] Y. Gong, J. Lin, X. Wang, G. Shi, S. Lei, Z. Lin, X. Zou, G. Ye, R. Vajtai, B. I. Yakobson, H. Terrones, M. Terrones, B. K. Tay, J. Lou, S. T. Pantelides, Z. Liu, W. Zhou, and P. M. Ajayan, *Vertical and in-plane heterostructures from WS_2/MoS_2 monolayers*, Nature Mater. **13**, 1135 (2014).

[82] R. B. Wilson and D. G. Cahill, *Anisotropic failure of Fourier theory in time-domain thermoreflectance experiments*, Nature Comm. **5**, 5075 (2014).

[83] J. Liu, G.-M. Choi, and D. G. Cahill, *Measurement of the anisotropic thermal conductivity of molybdenum disulfide by the time-resolved magneto-optic Kerr effect*, J. Appl. Phys. **116**, 233107 (2014).

[84] L. E. Reichl, *A Modern Course in Statistical Physics*, 2 edition ed. (Wiley-VCH, New York, 1998).

[85] R. K. Pathria and P. D. Beale, *Statistical Mechanics, Third Edition*, 3 edition ed. (Academic Press, Amsterdam ; Boston, 2011).

Paper I

Paper II

Paper III